

Surface chemistry of carbon dioxide

H.-J. Freund

*Physical Chemistry, Ruhr-Universität Bochum, 44780 Bochum, Germany
and*

Fritz-Haber-Institut der Max-Planck-Gesellschaft, Faradayweg 16, 14195 Berlin, Germany

and

M.W. Roberts

Department of Chemistry, University of Wales, Cardiff, CF1 3TB, UK



ELSEVIER

Amsterdam–Lausanne–New York–Oxford–Shannon–Tokyo

Contents

1. Introduction	227
1.1. Thermodynamic considerations	229
1.2. Bonding in CO ₂ : theory, computations and transition metal complexes	230
1.3. Intermolecular interaction and CO ₂ aggregate formation	235
2. Early spectroscopic and classical studies of CO ₂ adsorption	235
3. Structural studies of CO ₂ adsorbates	239
4. Adsorption of CO ₂ on metal surfaces	242
4.1. Adsorption of CO ₂ at sp-metal surfaces	242
4.2. Interaction of CO ₂ with transition metal single crystals	245
4.3. Adsorption of CO ₂ at copper surfaces	254
5. Chemisorption of CO ₂ at oxide surfaces	255
6. Reactions of CO ₂ with coadsorbed species	258
7. Alkali metal activation of CO ₂ at metal surfaces	263
8. Summary and conclusions	267
Acknowledgements	269
References	269



ELSEVIER

Surface Science Reports 25 (1996) 225–273

surface science
reports

Surface chemistry of carbon dioxide

H.-J. Freund^{a,b,*}, M.W. Roberts^c

^a *Physical Chemistry, Ruhr-Universität Bochum, 44780 Bochum, Germany*

^b *Fritz-Haber-Institut der Max-Planck-Gesellschaft,
Faradayweg 16, 14195 Berlin, Germany*

^c *Department of Chemistry, University of Wales, Cardiff, CF1 3TB, UK*

Manuscript received in final form 23 May 1996

Abstract

The review discusses how CO₂ surface chemistry has developed since the early 1950s. Emphasis is given to studies of well-characterized surfaces of metals, oxides and some more complex systems involving in particular alkali modified surfaces and also of coadsorbed molecules.

1. Introduction

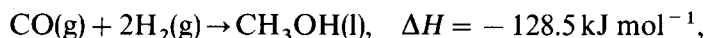
Even though CO₂ is both very abundant and a cheap C1 feedstock, at present it is only used in four industrially relevant technical processes [1]:

- (a) CO₂ interaction with ammonia leads to the important nitrogen containing nutrient, urea;
- (b) salicylic acid which is used in the production of pharmaceuticals and pesticides, etc. is formed by the “Kolbe–Schmitt” process from CO₂ and sodium phenolate;
- (c) cyclic organic carbonates are synthesized from CO₂ and epoxides which are used as solvents or in the production of polyacryl “fibres”;
- (d) methanol synthesis involves CO₂ through the water gas-shift reaction. It was the realization that CO₂ participated in synthesis that led to recent interest in CO₂ surface chemistry.

The main reason for the limited use of CO₂ as a chemical reactant is its rather low energy content as compared, for example, with carbon monoxide [2]. However, when reactive hydrogen is used as coreactant and the second oxygen in CO₂ is used to produce a stable product, as for example H₂O,

* Corresponding author. Tel.: +49-30-84134102; fax: +49-30-84134101; e-mail: freund@fhi-berlin.mpg.de.

the thermodynamics are much more favourable [3].



Therefore, thermodynamic arguments alone are not sufficient to explain the limited use of CO_2 in technical processes – the reasons are more likely to be kinetic in origin. One possibility that has emerged to overcome the kinetic barrier is to allow interaction of the molecule with a metal complex in a homogeneous reaction or with a solid or a biological surface in heterogeneous reactions. A comprehensive overview of CO_2 activation by metal complexes has been given by Behr [4]. In nature, CO_2 fixation occurs through photosynthesis at the biological surface of the enzyme ribulose 1,5-biphosphate carboxylase/oxygenase (Rubisco). It is clear that the active site is a Mg(II) ion embedded in a complex ligand field with oxygen atoms directly coordinated to the Mg centre [5]. Overviews of CO_2 activation in other biologically relevant processes as well as in heterogeneous catalysis, in electrochemistry and other fields have been given [6,7], with Solymosi [8] recently providing a comprehensive review of CO_2 interaction with clean and modified single crystal metal surfaces and related work on real catalyst surfaces.

In this review we discuss experimental surface studies in the context of theoretical work and various methodological approaches to tailoring the chemical reactivity of CO_2 towards a more effective use as a C1 feedstock in catalytic reactions.

In the early 1980s there was, partly due to the oil crisis, considerable impetus for investigating the potential of carbon dioxide as a reactant in hydrocarbon synthesis. A contributory factor was the claim that in methanol synthesis using CO , CO_2/H_2 mixture and the ICI copper supported on zinc oxide catalyst, CO_2 (not CO) was the main source of methanol. More recently carbon dioxide has been cited as one of the molecules that might enhance the green house effect and contribute to global warming. There are two options available, either ensure that CO_2 emission into the atmosphere is reduced through catalytic control or turn to advantage the availability of CO_2 generated in industrial processes through using it as a raw material for novel routes to useful chemicals.

There is no doubt that it is the thermodynamic stability of CO_2 (see Section 1.1) that contributed to the general lack of interest shown in the molecule's chemistry. Both terms (ΔS and ΔH) of the Gibbs free energy (ΔG) are not favourable for converting CO_2 to other molecules. The carbon–oxygen bonds are relatively strong and substantial energy has to be supplied for their cleavage, as we shall see further below. The entropy contribution through the term ($-T\Delta S$) makes little contribution to the thermodynamic driving force for any reaction involving CO_2 so that the value of the enthalpy change ΔH is a good guide to thermodynamic feasibility.

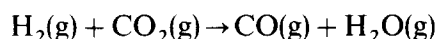
It is clear that progress in the use of CO_2 as a useful reactant will only emerge through the judicious use of novel catalytic chemistry. A positive change in free energy however should not be taken as a sufficient reason for not pursuing a potentially useful reaction involving CO_2 , the kinetics might indeed be favourable, ΔG only providing information on the yield at equilibrium through the relationship $\Delta G = -RT \ln K$. Provided that the kinetics are favourable CO_2 reduction may also be possible at metal surfaces where the free energy of oxide formation is highly favourable. The case of interaction with zirconium is a case in point [9], the reaction $\text{Zr} + 2\text{CO}_2\text{(g)} \rightarrow \text{ZrO}_2 + 2\text{CO(g)}$ occurring readily at high temperatures; a further example is CO_2 dissociative chemisorption at molybdenum surfaces where surface carbide and oxide occurs at 295 K [10,11].

1.1. Thermodynamic considerations

Any attempt to use CO₂ as a chemical feedstock must take into account its relative stability. Thermodynamics provides us with information to discuss phenomenologically the issue in terms of the Gibbs–Helmholtz relationship

$$\Delta G = \Delta H - T\Delta S.$$

The formation of CO and oxygen from CO₂ is associated with a large positive ΔH (293.0 kJ mol⁻¹). However a more favourable enthalpy of reaction under standard conditions (1 atm pressure for each product or reactant and 298 K temperature) can be achieved if less stable reactants and more stable products are involved. For example, the hydrogenation of CO₂ is thermodynamically more favourable with $\Delta H^\ominus = +41.2$ kJ mol⁻¹. The reverse water gas-shift reaction could be operated under

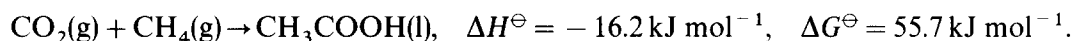


conditions which allow the entropy term to dominate; for example at 1500 K the reaction becomes slightly exergonic ($\Delta G^\ominus = -1.07$ kJ mol⁻¹). In Table 1 we compare the thermodynamic terms (kJ mol⁻¹) for several reactions with the reverse water gas-shift reaction at room temperature (see Schmidt in [6]).

Hydrocarbons can also be used as reductants and the thermodynamics of such reactions are as follows [6]:



or



While the reforming reaction to produce syngas (above) has been studied by several groups [12,13] and challenges have been discussed, the reaction to form acetic acid from CO₂ and methane (above) has not generally been considered. However, recently, interest has increased in this reaction [14,15]. For the former, reaction technologies namely the SPARG process [16] and the CALCOR process [17], which target different markets, have been developed. Both processes address the problem of coke formation and catalyst stability by catalyst modification and high working temperatures (> 900°C). Also methanol synthesis from CO₂ and H₂ is being actively pursued [18] including through the EC supported project at Bochum, Cardiff, Düsseldorf and Rome.

Table 1
Thermodynamics of reactions involving CO₂

	ΔH^\ominus	$-T\Delta S^\ominus$	ΔG^\ominus
$\text{H}_2(\text{g}) + \text{CO}_2(\text{g}) \rightarrow \text{CO}(\text{g}) + \text{H}_2\text{O}(\text{g})$	41.20	22.6	18.60
$\text{H}_2(\text{g}) + \text{CO}_2(\text{g}) \rightarrow \text{CO}(\text{g}) + \text{H}_2\text{O}(\text{l})$	-2.80	22.8	20.00
$\text{H}_2(\text{g}) + \text{CO}_2(\text{g}) \rightarrow \text{HCOOH}(\text{l})$	-31.20	64.2	33.00
$2\text{H}_2(\text{g}) + \text{CO}_2(\text{g}) \rightarrow \text{CH}_2\text{O}(\text{g}) + \text{H}_2\text{O}(\text{l})$	-9.00	55.0	44.00
$3\text{H}_2(\text{g}) + \text{CO}_2(\text{g}) \rightarrow \text{CH}_3\text{OH}(\text{l}) + \text{H}_2\text{O}(\text{l})$	-131.30	122.1	-9.20
$4\text{H}_2(\text{g}) + \text{CO}_2(\text{g}) \rightarrow \text{CH}_4(\text{g}) + 2\text{H}_2\text{O}(\text{l})$	-252.90	122.1	-130.80

1.2. Bonding in CO_2 : theory, computations and transition metal complexes

CO_2 in its electronic ground state is a closed shell linear system with ${}^1\Sigma_g^+$ symmetry [19]. Its electronic structure may be represented by a molecular orbital diagram as shown in Fig. 1. On the right-hand side, schematic drawings of the molecular orbitals in a sequence as revealed by an ab initio Hartree–Fock calculation [20] are shown, however, not to the energy scale. The atomic orbitals on carbon and oxygen which are important in bond formation are 2s and 2p. In the linear molecule six atomic orbitals consisting of 2s and $2p_z$, directed along the molecular axis, mix to give six molecular orbitals of σ symmetry. These are labelled $3\sigma_g$, $4\sigma_g$, $5\sigma_g$ and $2\sigma_u$, $3\sigma_u$, $4\sigma_u$. The three 1s atomic orbitals are basically unchanged in the molecule and become $1\sigma_g$, $2\sigma_g$ and $1\sigma_u$. The $2p_x$ and $2p_y$ orbitals form three doubly degenerate π -orbitals labelled $1\pi_g$, $1\pi_u$ and $2\pi_u$. The $1\pi_g$ molecular orbital cannot contain any contribution from the carbon atom as the 2p atomic orbitals on the oxygen atoms are out of phase. The π -orbital energies increase with the number of nodal planes and they are arranged accordingly in Fig. 1.

CO_2 contains 22 electrons of which six occupy the core 1s orbitals. The remaining 16 valence electrons are distributed over four σ orbitals (eight electrons) and two π -orbitals (eight electrons). The highest occupied molecular orbital is the $1\pi_{gx}$ orbital, the lowest unoccupied molecular orbital is

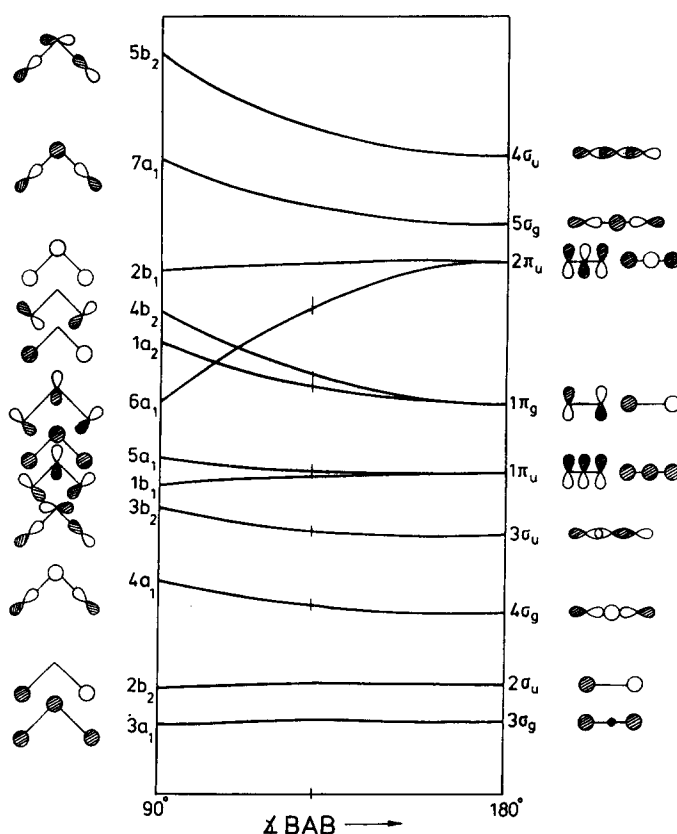


Fig. 1. Walsh diagram of CO_2 orbital energies in linear and bent geometries.

the $2\pi_u$ orbital. The six occupied orbitals may be classified as two σ -C-O bonds ($3\sigma_g, 2\sigma_u$) and two σ lone pairs ($4\sigma_g, 3\sigma_u$). The $1\pi_u$ represents the π -C-O bonds and $1\pi_g$ the π lone pairs. In order to judge the stability of the linear geometry, Fig. 1 shows, in a qualitative way, the energy positions of the occupied and unoccupied orbitals upon bending the linear geometry [21]. It is obvious that all σ -orbital energies increase slightly or are unchanged from the linear to the bent configuration. In contrast, the π -orbital energies show pronounced alterations. In the bent molecule the degeneracies of all the π -orbitals are split. This is clear from Fig. 1, if we remember the two equivalent components in and perpendicular to the plane of the paper. If the molecule bends in the plane of the paper (Fig. 1), the energies of each molecular orbital are no longer equal. As Fig. 1 shows, the splitting is not very large for $1\pi_u$ and $1\pi_g$. However, for the $1\pi_g$ the energies of both components increase indicating that the linear geometry is more favourable for the orbitals. For the $2\pi_u$, one component becomes the $2b_1$ orbital (in plane) with energy almost unchanged upon bending. But the energy of the other component of $2\pi_u$ (out of plane) falls sharply in the bent molecule, becoming the $6a_1$ orbital. Mixing of the $6a_1$ molecular orbital with other bonding molecular orbitals of the same symmetry, leads to the introduction of s character in $6a_1$ and to an appreciable lowering of energy. Occupation of the $2\pi_u-6a_1$ molecular orbital is particularly important in determining the bond angle, since this is the only valence orbital for which the bent molecule is strongly favoured. We may imagine that processes at surfaces involve electron transfer from a substrate into the CO_2 molecule which in turn would lead to occupation of this orbital via the formation of a CO_2^- anion. On the basis of the Walsh diagram [21] shown in Fig. 1, we would expect such an anion to be bent in its equilibrium geometry. If the charge transfer goes in the other direction, namely from the CO_2 molecule to the substrate, we would have to consider the formation of a CO_2^+ cation, which would, according to Fig. 1, remain in the linear geometry. However, any excitation across the HOMO-LUMO gap in the CO_2 molecule will lead to excited states of the CO_2 molecule with a tendency for the molecule to bend. Parallel to ionization and/or excitation the bonding properties within the molecule are considerably changed. Fig. 2 summarizes energetic as well as spectroscopic properties of the neutral and ionized species and relates them to those of possible simple reaction products such as CO, carbon and oxygen [22–26].

It is clear from Fig. 2 that an energetically favoured reaction will involve the anionic species. All other processes require energies which are orders of magnitude larger than those involving CO_2^- . It is therefore important in the context of the present study to consider the formation of CO_2^- in the gas phase in more detail. CO_2^- is metastable against autodetachment of the electron [27,28]:



with an activation barrier of 0.4 eV. The anion has an average life time of 60–90 μs [27,28]. This means, the anion may be identified spectroscopically after it has been formed either by electron scattering or by other means such as irradiation of formates [29,35]. The reason for the relatively high stability of the anion is the barrier due to the change in molecular geometry. Fig. 3 shows a schematic potential energy surface of the electron attachment process [31], the schematic potential energy diagram of CO_2 and CO_2^- being plotted as a function of the C-O distance and the O-C-O bond angle. The ground state of the CO_2 system is shown at $R_{\text{CO}} = 1.15 \text{ \AA}$ representing the linear system with an enthalpy of formation of $-1650 \text{ kJ mol}^{-1}$ [2]. The double-well ground state of the CO_2^- at $R_{\text{CO}} = 1.24 \text{ \AA}$ represents a bent geometry with elongated C-O bonds and an enthalpy of formation $-1604 \text{ kJ mol}^{-1}$, i.e. about 0.5 eV higher than linear CO_2 [26]. This value corresponds to the adiabatic electron affinity of CO_2 (Fig. 2) in contrast to the vertical affinity which is considerably

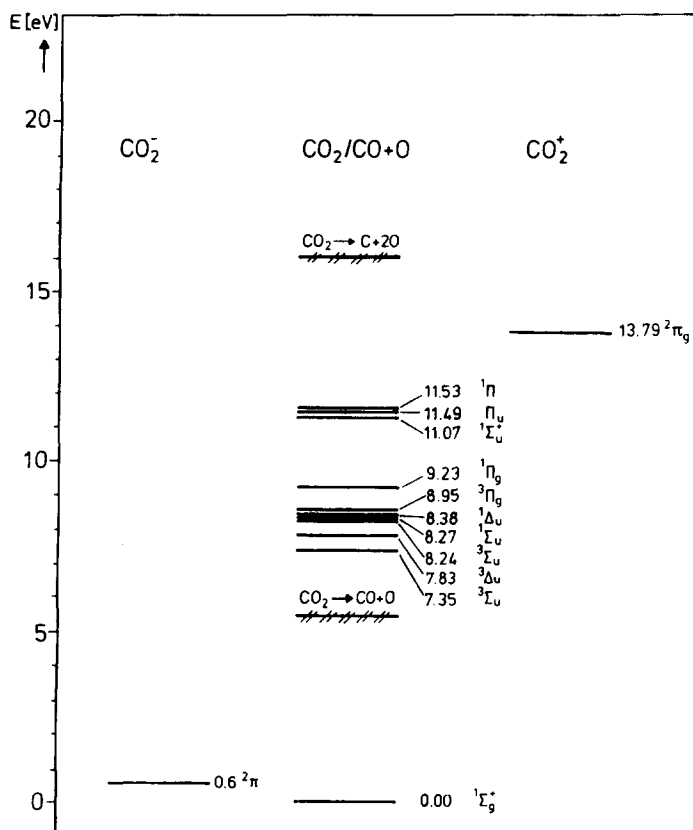


Fig. 2. Total energy differences of various ground and excited states of CO_2 neutral, cationic and anionic. Dissociation energies of neutral CO_2 into CO and oxygen as well as carbon and oxygen are indicated.

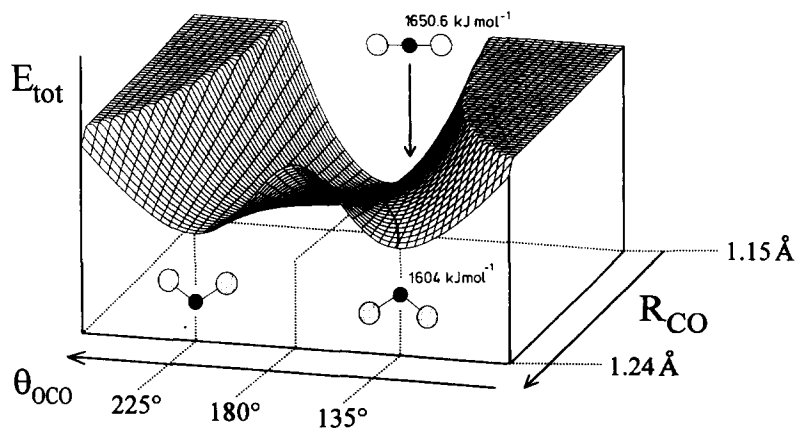


Fig. 3. Schematic potential energy diagram connecting linear neutral CO_2 with bent anionic CO_2^- . Experimentally determined energies are given in kJ mol^{-1} .

higher [32]. The CO_2^- molecule in its equilibrium geometry is thus thermodynamically metastable, but stabilized kinetically. The vibrational spectrum of CO_2^- is known [33] and can be used by comparison with linear CO_2 as a fingerprint to identify the CO_2^- species. Similarly, the photoelectron spectrum of gaseous CO_2 [24], which has been determined, can be compared with the calculated spectrum of CO_2^- [34] and used to identify an anionic adsorbed species. Fig. 4 shows the observed photoelectron spectra in the gas [35] and in the condensed phase [36,37] together with calculations of decreasing degree of sophistication [34,38]. Calculations including the effect of relaxation and correlation in the hole state do reproduce satisfactorily the observed ionization energies, while Koopmans energies only give a qualitative account of the sequence and energies of the ion states [34]. However, in the present case the Koopmans representation is sufficient to judge qualitatively how the ionization energies change upon CO_2^- formation. In the CO_2^- case the experimental spectrum of the gas phase species is not known. We expect of course a splitting of the π -states due to breaking of the symmetry. The correlation between the CO_2 and CO_2^- states is given in Fig. 4. We may use this information in an assignment of the spectrum of adsorbed species [39]. The changes of the stretching frequencies are particularly pronounced and may be used as fingerprints. The lower values reflect the smaller average bond order of the C–O bond which is only 1.5 in CO_2^- as compared with 2 for CO_2 . This is also in line with the smaller bond enthalpy of the C–O bond in CO_2^- which therefore is more unstable against dissociation.

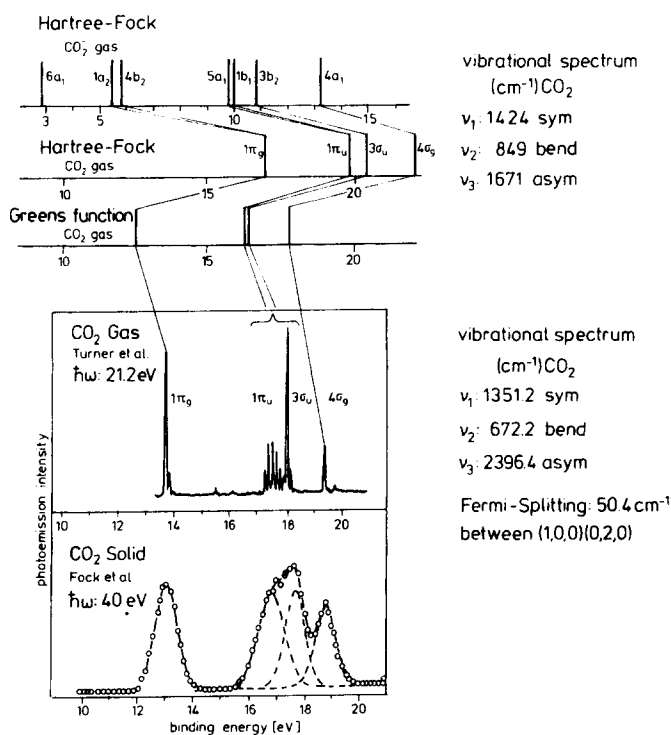


Fig. 4. Comparison of measured (gas phase [35] and condensed phase [36,37]) photoelectron spectra of CO_2 with calculations [34,38]: The calculated ionization energies of CO_2^- [34] as well as the vibration energies in neutral and anionic CO_2 are given.

CO₂ is a molecule with several possible modes of coordination [40]. Fig. 5 schematically summarizes the observed structures. They may be classified as due to coordination of the geometrically undistorted CO₂ molecule to one or several metal centres, or as the coordination of a bent CO₂ anion to one or several metal centres.

One might imagine that the undistorted molecule exhibits two bonding modes, namely via the oxygen atom(s) forming a linear CO₂–metal bond or via the π-bonds of the CO₂ molecule. In comparison with this, the bent molecule could exhibit three modes of coordination: (a) a pure carbon coordination, or (b) a pure oxygen bidentate coordination, or (c) a mixed carbon–oxygen coordination. A large number of CO₂ transition metal complexes have been synthesized but only a few have been characterized structurally via X-ray scattering [41–44]. Typical bond lengths in the respective systems are given in Fig. 5. It is remarkable to note that structural characterizations have only been reported for bent CO₂ coordinated to one or several metal centres. Typical examples are shown in Fig. 5 [41–44]. The coordination mode in which only the oxygen atoms are involved in the bonding has not been experimentally verified for transition metal complexes. Also, the example shown for the pure carbon coordination [44] is probably stabilized via interaction of the oxygen atoms with the surrounding ligands.

However, several quantum chemical *ab initio* calculations have been reported on the interaction of a CO₂ moiety with a single metal atom [34,45–47]. In general it is found that the mixed carbon–oxygen, as well as the pure oxygen coordinations, lead to more stable arrangements than the

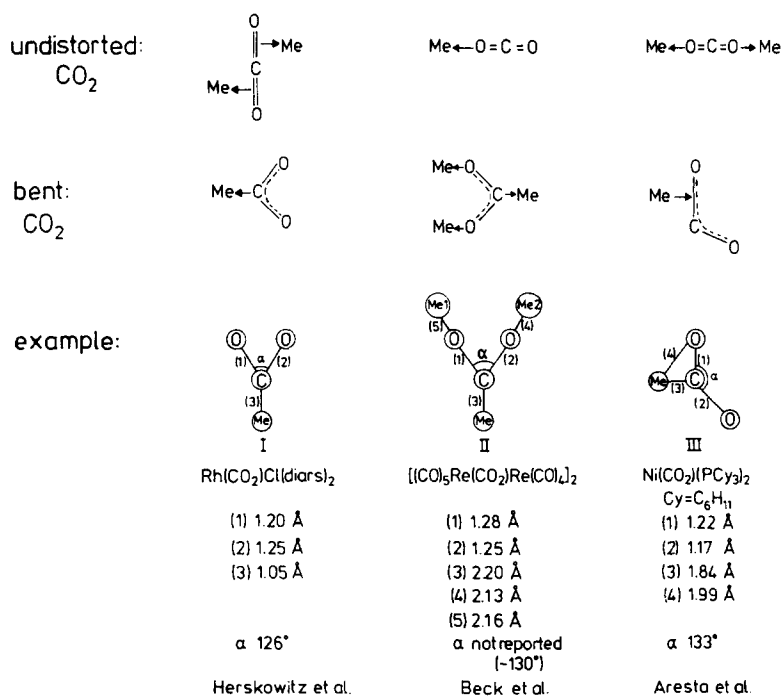


Fig. 5. Modes of coordination of neutral and anionic CO₂ are schematically given. Experimental geometries from X-ray structure determinations are given for comparison [41,42,44].

pure carbon coordination. In any case the bond is always characterized as the coordination of a CO_2^- (bent) to a metal cation. The two coordinate bonds of the oxygen atom yield more stabilization than the single C–metal bond [34].

1.3. Intermolecular interaction and CO_2 aggregate formation

Carbon dioxide has a relatively large quadrupole moment (-3.2 a.u.) [48] and thus exhibits strong intermolecular interaction. These interactions become even stronger when an ionized atomic or anionic molecular CO_2 moiety interacts with other neutral CO_2 molecules forming intermolecular aggregates. These latter aggregates may be viewed as models for a solvated cationic or anionic species [49–53].

In the case of the neutral aggregates information on stability and structure has been gained by molecular beam electric resonance spectrometry [49]. It is relatively easy to produce $(\text{CO}_2)_n$ clusters with $2 \leq n \leq 5$ in a molecular beam expansion system and observe them via mass spectrometry. In a so-called refocussing experiment the question whether a molecule is polar or non-polar may be investigated. For the simplest case of the CO_2 dimer the question whether the geometry is parallel or a T-shaped arrangement has not been completely clarified experimentally, but there are very strong indications that the molecule is polar pointing towards a T-shaped arrangement. Calculations support this assignment only partly, in the sense that the two possible structures exhibit very close energies [51].

Positively charged cluster ions $(\text{CO}_2)_n^+$ with $2 \leq n \leq 10$ may be synthesized by nucleation of neutral CO_2 molecules to the cationic monomer in a superionic expansion [50]. The stability of these clusters is considerably higher than those of the neutrals. The first neutral CO_2 is bound by 11.8 kJ mol^{-1} to the CO_2^+ cation, the second CO_2 molecule to the $(\text{CO}_2)_2^+$ by 13.8 kJ mol^{-1} , the third CO_2 molecule to the $(\text{CO}_2)_3^+$ by 11.7 kJ mol^{-1} , etc. supporting the idea of a charged dimer within a neutral cluster.

Parallel to the relatively high stability of the cationic clusters, the anionic clusters are also rather stable [52]. In fact, while the monomer CO_2^- is unstable with respect to electron detachment, the $(\text{CO}_2)_2^-$ dimer appears to be stable by 0.9 eV and the stability increases with increasing cluster size. The implications of this experimental finding are rather important for the present review in the sense that electron transfer from a substrate towards CO_2 will be facilitated via solvation of the formal anionic species. Studies at low temperatures may therefore favour CO_2^- formation when CO_2 clusters are likely.

There is relatively little known experimentally about the structures of the ionic clusters. Calculations suggest T-shaped structure for the cationic as well as for the anionic clusters [53]. In the latter case, of course, the T-shaped structure is formed from a bent CO_2^- anion which interacts via an oxygen atom with a basically undistorted CO_2 molecule as shown in Fig. 6.

2. Early spectroscopic and classical studies of CO_2 adsorption

Eischens and Pliskin in 1957 [54] reported IR spectra for CO_2 adsorbed on a Cabosil supported Ni catalyst and also with NiO. Fig. 7(a) shows the spectra recorded for the two substrates at about 1 Torr pressure of CO_2 in the IR cell in the $1350\text{--}1700 \text{ cm}^{-1}$ range and in the range of $2280\text{--}2400 \text{ cm}^{-1}$ for 200 Torr pressure at room temperature (Fig. 7(b)). The assignments are shown in the

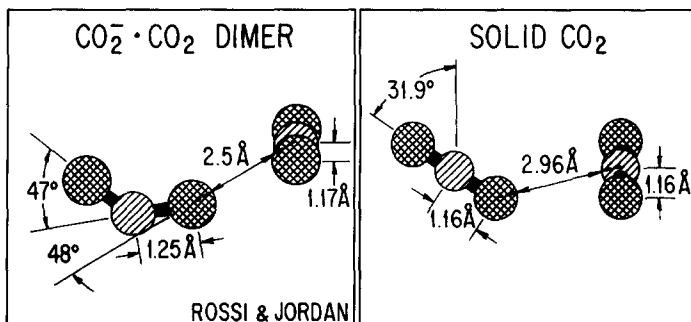


Fig. 6. Schematic diagram of the intermolecular arrangement of CO_2 moieties in the $(\text{CO}_2)_2^-$ dimer anion as compared with solid CO_2 .

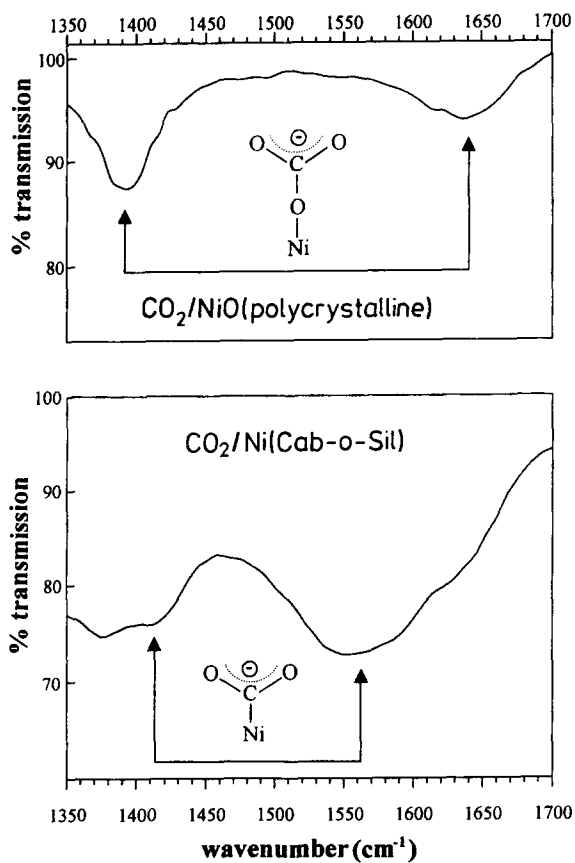


Fig. 7. Infrared spectra reported by Eischens and Pliskin [54] redrawn onto a wave number scale: (a) CO_2 on Ni cabosil and NiO(poly) under 1 Torr pressure at room temperature.

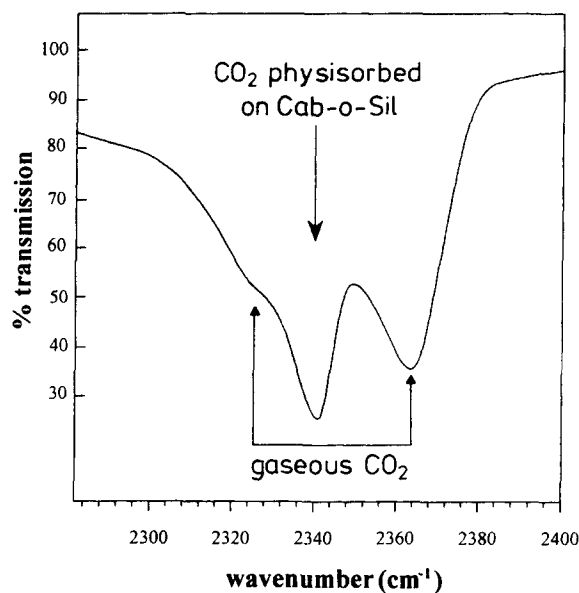


Fig. 7. (b) CO₂ physisorbed on NiO(poly) at 200 Torr pressure at room temperature.

figure. The bands at 1555 and 1415 cm⁻¹ were assigned to a nickel carboxylate, while the bands at 1640 and 1405 cm⁻¹ were attributed to the formation of carbonate species from CO₂ and coadsorbed residues of oxygen. If the supported Ni is exposed to CO₂ at a temperature of 100°C, bands associated with adsorbed CO are detected, indicating CO₂ reduction and/or contamination by CO inadvertently present. The assignments of the carbonate bands is supported by the spectra observed after CO₂ adsorption on the NiO samples. In fact, the observation of two bands in the appropriate energy regime led Eischens and Pliskin to propose the formation of a monodentate carbonate, because they argued that a symmetric CO₃ anion should only exhibit one single band. Before considering further this conclusion, we mention that the bands observed in the region 2320–2380 cm⁻¹ are due to a mixture of physisorbed and gaseous CO₂ [54]. Blyholder and Neff [55], considerably later, reported results for silica supported iron which seem to indicate CO formation at room temperature suggesting dissociative chemisorption of CO₂. They also observed the appearance of bands due to physisorbed CO₂.

These studies initiated two lines of investigations: one was concerned with detailed investigations of the carbonate bands, the other with the study of the nature of the metal carboxylate band formed in CO₂ adsorption on the clean metal surface.

In 1958 Gatehouse et al. [56] studied the IR spectra of a variety of carbonates of different bonding character and symmetry. On the basis of the normal mode analysis by Fujita et al. [57] for a cobalt (III) carbonate complex and a series of studies by various laboratories, Little in his important book "Infrared spectra of adsorbed species" [58] systematized the carbonate bands as shown in Fig. 8. For a symmetrical CO₃ anion we expect a symmetrical stretching mode at 1063 cm⁻¹ and a degenerate asymmetric stretching mode at 1415 cm⁻¹. The lowest energy band is due to an out-of-plane bending π -mode of the CO₃ anion. The important message is that the degenerate asymmetric band splits in a characteristic way depending on coordination and bond character. While in a monoden-

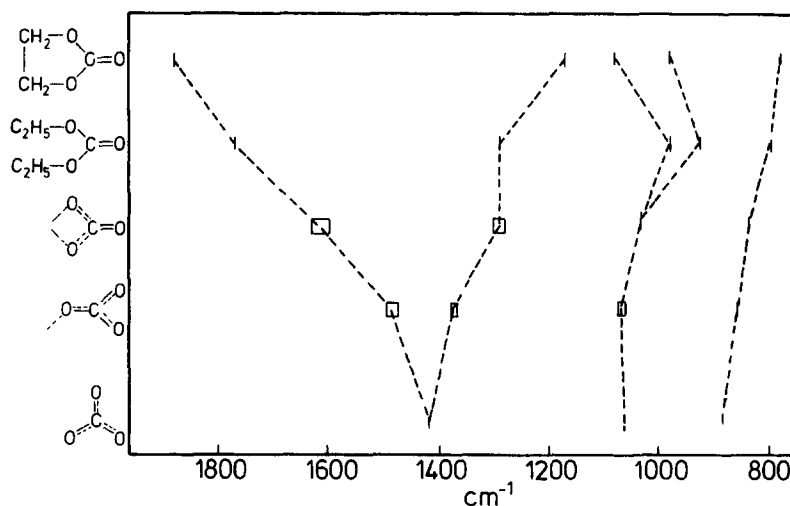


Fig. 8. Correlation diagram of characteristic CO_3 vibration frequencies in various bonding modes after Little [58].

tate situation the splitting is small, it increases in bidentate coordination with an even further increase in covalently bonded (strained) organic carbonates. On the basis of such systematics, it was possible to classify results observed with various oxide catalysts and we refer the reader for details to the literature [59–61].

Earlier, and parallel to the work of Eischens and Pliskin [54], studies of CO_2 interaction with metal surfaces were reported. The results were conflicting. As early as 1951 Crowell and Farnsworth [62] found that a small fraction of a nickel single crystal surface irreversibly adsorbed CO_2 in the temperature range up to 500 K, while other workers did not detect any adsorption on electrolytically polished Ni surfaces [63]. Collins and Trapnell [64] found irreversible CO_2 adsorption on evaporated Ni films at 200 K, while Hayward and Gomer [65] concluded that with tungsten CO_2 dissociates to CO and oxygen at temperatures up to 900 K. From these measurements these authors deduced a heat of adsorption of CO_2 of 750 kJ mol^{-1} for “clean” tungsten surfaces.

Subsequent to the report by Eischens and Pliskin for the formation of nickel carboxylate in CO_2 adsorption, a series of publications from different laboratories on this subject were published. Eischens and Pliskin [66] as well as Quinn and Roberts [67] concluded from their studies that CO_2 dissociates at room temperature at nickel to give chemisorbed CO and oxygen. In 1962 Suhrmann et al. [68] published an interesting study of CO_2 adsorption on Ni at various temperatures. Their work function measurements at 77 K indicated a pronounced increase, depending on the preparation conditions, up to the completion of a monolayer. Admission of further CO_2 led to a decrease in the work function. At a temperature of 77 K (Fig. 9) the situation is similar except that the work function maximum is shifted to higher coverages. At 195 K the maximum of the work function could not be observed with the methods applied. The conclusion was that there is an increase in work function corroborating the idea of a metal carboxylate with a dipole whose negative end points away from the surface. Also, the dissociation of CO_2 at room temperature is compatible with these data. We shall see below that more recent studies with single crystal Ni surfaces show many aspects that are in accord with these conclusions.

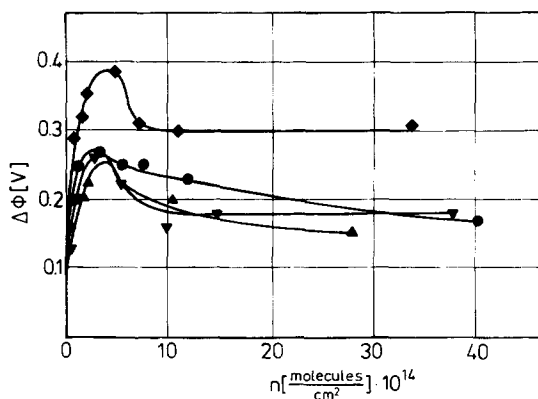
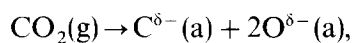


Fig. 9. Work function changes after exposing a Ni film to CO_2 at 77 K. $\circ, \Delta, \nabla, \diamond$: four experiments to judge reproducibility (after [68]).

The emergence of electron spectroscopy coupled with ultra high vacuum techniques in the early 1970s provided an opportunity to explore further the state of adsorbed CO_2 at metal surfaces [69]. The physical adsorption of CO_2 on gold at 80 K was one of the first to establish the surface sensitivity of XPS and UPS for the study of molecules adsorbed at metal surfaces [69]. Furthermore carbon dioxide (with carbon monoxide) was used as model systems to explore whether XPS and UPS could discriminate between molecular and dissociative regimes of adsorption [11]. The O(1s) peak characteristic of physically adsorbed CO_2 at a gold surface was at 533 eV while the corresponding orbital energies were (using He I radiation) at 6.9, 9.6, 11.0 and 13.1 eV. These compare with values of 13.7, 17.6, 18.0 and 19.4 eV for gaseous CO_2 but which have to be corrected since the adsorbed state is referenced to the Fermi level of the gold substrate. The correction is ~ 7 eV in this case. Adsorption of CO_2 at molybdenum at 77 K gave rise to two O(1s) peaks, that at 533 eV was assigned to molecularly adsorbed CO_2 the intensity of which decreased rapidly on warming and was negligible at 200 K. The second O(1s) peak at 77 K was at a binding energy of ~ 530 eV; the intensity of this peak increased on warming and was the only one present at 295 K. Adsorption of CO_2 directly at 295 K gave rise to just the single O(1s) feature at 530 eV and a C(1s) peak with a binding energy of 283 eV. The conclusion was that with molybdenum the carbon dioxide was dissociatively chemisorbed [11] at room temperature to generate surface carbide and oxide characterized by C(1s) and O(1s) binding energies of 283 and 530 eV,



respectively. Adsorption of carbon monoxide was also characterized by similar C(1s) and O(1s) values at 295 K and indicative of dissociative chemisorption [11].

3. Structural studies of CO_2 adsorbates

Information on adsorbate geometries, including interatomic distances, has been collected using electron diffraction methods, and in particular LEED and diffuse LEED (DLEED) [70]. Other spectroscopic methods such as ARUPS [71] and NEXAFS [72] have also been applied. In the latter,

polarized light has been used to determine the symmetry of adsorption sites and thus deduce structural parameters while electron energy loss spectroscopy (HREELS) has been employed to determine adsorbate symmetries [73]. These methods have been mainly applied to $\text{CO}_2/\text{Fe}(111)$ [74–76] and $\text{CO}_2/\text{Ni}(110)$ [39,77]. Fig. 10 summarizes the situation for $\text{CO}_2/\text{Ni}(110)$ and shows the NEXAFS spectra near the oxygen K-edge. On the left of Fig. 10 are shown the spectra at low temperatures [77]. The three features in the spectrum are due to coadsorbed neutral physisorbed CO_2 and partially negatively charged chemisorbed $\text{CO}_2^{\delta-}$. The spectra are recorded as a function of the polar angle θ as defined in the inset. The chemisorbed species give rise to clearly pronounced π - and σ -resonances while the σ -resonance of the physisorbed species is very weak. Due to the overlap

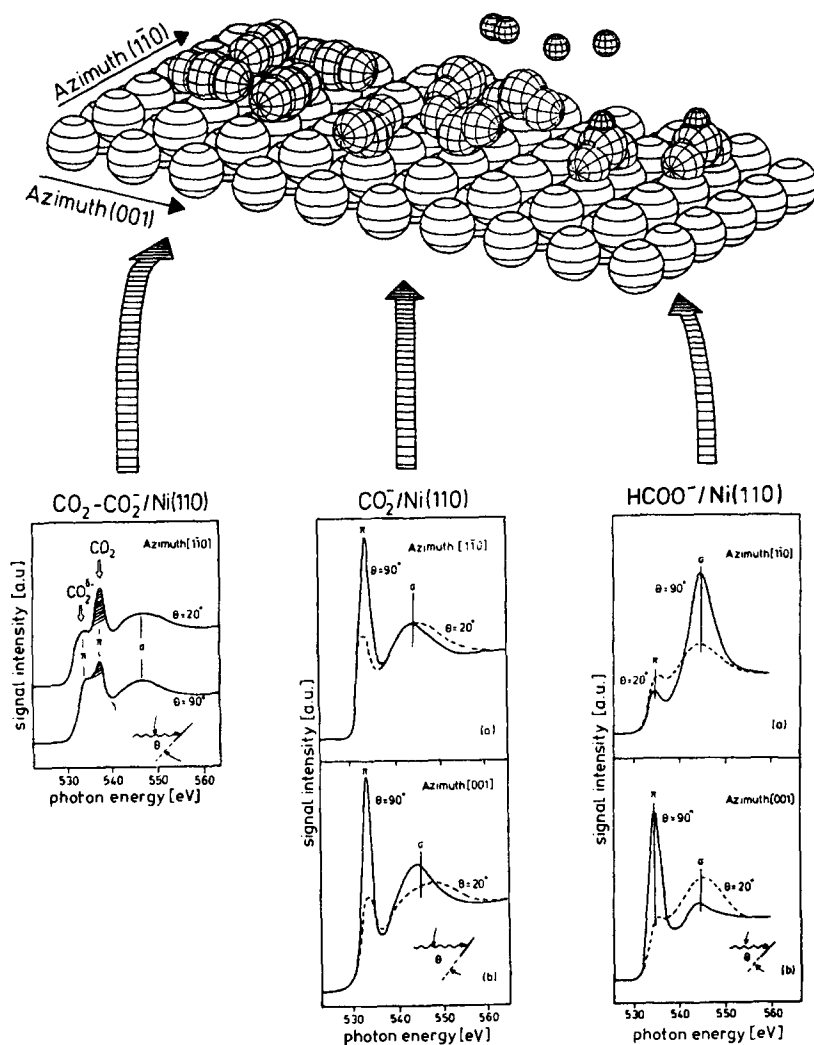


Fig. 10. Collection of NEXAFS spectra at the oxygen edge of CO_2 and HCO_2^- adsorbates on $\text{Ni}(110)$ at 77 K. Polar angle of light incidence and azimuth are given. In the top panel the possible adsorbate structures are schematically represented.

of the features a structure determination is very difficult. However, if the substrate temperature is increased slightly one can selectively desorb the physisorbed species and study the isolated chemisorbed $\text{CO}_2^{\delta-}$ species. The NEXAFS data at this temperature are shown in the central panel. While the σ -resonance is independent of the polar angle, the π -resonance is strongly attenuated when the electric field vector is oriented perpendicular to the surface plane. Since the π -resonance corresponds to the excitation from the O(1s) orbitals into the lowest unoccupied π -orbital, the observed intensity variation is compatible with a molecular $\text{CO}_2^{\delta-}$ species oriented with its plane perpendicular to the substrate surface. We know from independent EELS data, to be discussed later, that the symmetry of the adsorbate site is probably C_{2v} , with the oxygen atoms interacting with the substrate. DLEED data, on the other hand, cannot differentiate between carbon and oxygen coordination. The present θ dependent NEXAFS spectra have been taken in two azimuths, i.e. parallel to the $(1\bar{1}0)$ and the (100) azimuths. As is clear from the experimental data there is no preferential orientation of the molecular plane along one of the two azimuths. This allows for two possibilities, namely a static adsorption model with no preferential orientation or a dynamical adsorption model, where the molecular plane rotates freely. So far, we cannot decide between these possibilities although temperature dependent measurements obviously going well below liquid nitrogen temperatures should allow a distinction to be made. Interesting changes occur when we “convert” $\text{CO}_2^{\delta-}$ to formate, i.e. by addition of a hydrogen atom to the $\text{CO}_2^{\delta-}$ carbon atom. The NEXAFS data for a formate adsorbate on Ni(110) are shown in the right-hand panel of Fig. 10 [78], the polar angle dependences are very similar to those observed for $\text{CO}_2^{\delta-}$ (a). However, in the case of the formate adsorbate there are clear dependences on the azimuth. The π -resonance is large when the electric field vector is oriented perpendicular to the $(1\bar{1}0)$ azimuth, indicating an orientation of the molecular plane parallel to the $(1\bar{1}0)$ azimuth. Since formate can only be coordinated to the surface via the oxygen atoms, the bonding must occur as indicated on the right-hand side of the adsorbate model. We do not know whether the molecule is coordinated to a single metal atom as a monodentate or to two atoms as a bidentate [78,79]. This comparison between $\text{CO}_2^{\delta-}$ and formate points very strongly towards carbon coordination for the $\text{CO}_2^{\delta-}$ chemisorbate, because this coordination would allow for free rotation about the carbon–metal bond. However, since the evidence from vibrational spectroscopy is rather strong for oxygen coordination also in the case of the $\text{CO}_2^{\delta-}$ chemisorbate, there is insufficient evidence for us to draw a final conclusion [80,81]. Beyond the system $\text{CO}_2/\text{Ni}(110)$ there is hardly any system for which comparable data are available. NEXAFS data have been recorded, on the other hand, for carbonate adsorbates [82–84]. Much of the work has been performed on silver substrates namely Ag(110). The carbonate species is readily formed by reaction of CO_2 with an oxygen precovered surface. It leads to an ordered LEED pattern with (1×2) symmetry [83,84]. Several surface spectroscopic methods have been applied to this particular structure and we discuss this further below focussing on structural aspects. Fig. 11 collects the C-K and O-K edge spectra reported by Madix et al. [82] in various excitation geometries as indicated. The dependence of the intensity of the $\text{C}(1s) \rightarrow \pi^*$ and $\text{C}(1s) \rightarrow \sigma^*$ transitions of the carbonate on the orientation of the electric field of the incident light indicates that the species lies in a plane parallel to the plane of the surface. The positions of the observed resonances agree with those of bulk carbonates (e.g. CdCO_3) [85] indicating similar bond lengths. The vibrational spectrum of this species reveals a C_s symmetry of the overall surface complex.

The conclusions based on the NEXAFS data are in the main corroborated by corresponding investigations using angle resolved photoelectron spectroscopy [86].

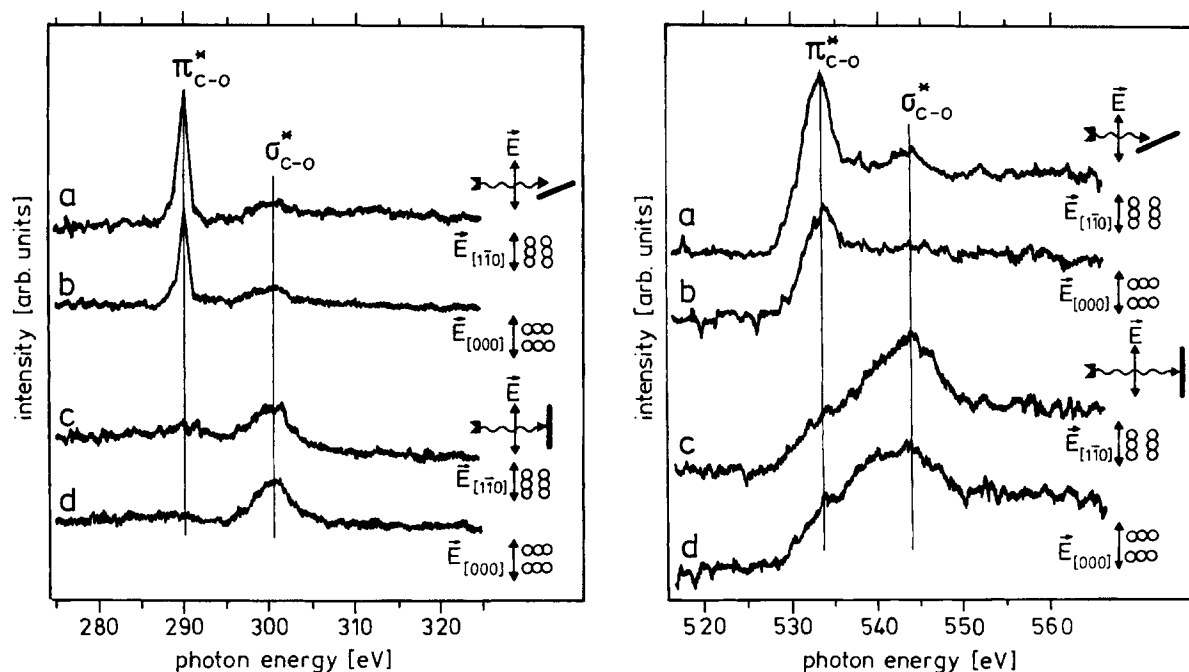


Fig. 11. NEXAFS spectra at the carbon and oxygen edges of carbonate (CO_3) adsorbed on $\text{Ag}(110)$. The geometries for recording the spectra are indicated (after [82]).

4. Adsorption of CO_2 on metal surfaces

4.1. Adsorption of CO_2 at *sp*-metal surfaces

Although the earlier XPS studies of CO_2 adsorption had indicated that the molecule dissociated at molybdenum film surfaces (Fig. 12) at low temperatures [11], other than characterization of the physically adsorbed state (Fig. 13) at gold [69], there was no information available on CO_2 's reactivity at *sp*-metal surfaces. What stimulated us to investigate aluminium and magnesium surfaces was that in both cases there was a strong thermodynamic driving force for oxide formation and therefore to dissociative chemisorption. Furthermore there were strong indications that the classical distinction between *sp*- and *d*-metals in chemisorption reactivity could not be sustained in that both $\text{Zn}(0001)$ and $\text{Mg}(0001)$ surfaces had been shown to dissociatively chemisorb nitric oxide at low temperatures [87].

The first report of a combined XPS and HREELS investigation of reactive CO_2 chemisorption was at a $\text{Mg}(0001)$ surface [88]. At 85 K only molecular adsorption is observed but on warming, reactive chemisorption occurs leading to surface carbonate and oxide and characterized by $\text{O}(1s)$ binding energies of 533 and 530.5 eV, respectively. The $\text{C}(1s)$ binding energy of the carbonate was at about 292 eV. The C:O atom ratio calculated from the relevant $\text{C}(1s)$ and $\text{O}(1s)$ peak intensities was 1:3.2 i.e. close to the 1:3 ratio of the carbonate species. By taking photoelectron spectra at different collection angles relative to the surface normal it was shown that carbonate and oxide have quite different distributions within the surface region with the carbonate being confined largely to the

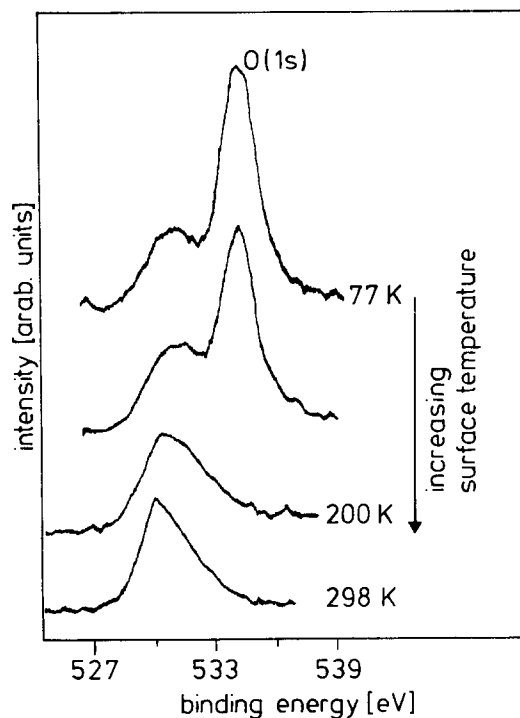


Fig. 12. O(1s) photoelectron spectra of CO₂/Mo(poly) as a function of surface temperature [11].

top-most atomic layer and the oxide present as an underlayer. The carbonate concentration was calculated to be $\sim 4 \times 10^{14} \text{ cm}^{-2}$ and the oxide to be about 0.4 nm thick. The main loss features in the HREEL spectrum were at 850, 1090, 1390 and 1630 cm^{-1} . Although these losses are in general agreement with what might be anticipated from carbonate species, it was not possible to judge whether either bi- or unidentate carbonate species were present or whether it was a mixture of both types.

At polycrystalline aluminium surfaces very similar molecular events were observed in that reactive chemisorption led to carbonate and oxide formation [89,90]. However, a feature of this work was the unusual temperature dependence of the chemistry (Fig. 14). At low temperatures (120 K) both carbonate and oxide formation occurred and on warming, the intensity of that associated with the oxide (531.8 eV) increased at the expense of that assigned to the carbonate (533.5 eV). This transfer of intensity continued as the temperature was raised (Fig. 14) to 295 K and was a clear indication for the reduction of the carbonate to surface oxide. The C(1s) spectra confirmed this in that there was a shift in the binding energy from initially at 291.3 eV (CO₃) to 285 eV (CO) and 282 eV (carbide).

It was, however, the unusual characteristics of the temperature dependence of the chemisorption reaction that was a significant feature of the aluminium–carbon dioxide system. At 295 K the surface was unreactive after extensive exposure to CO₂ (10 000 L) at a pressure of $\sim 10^{-6}$ Torr; however, on increasing the CO₂ pressure to 1 Torr there is extensive reaction at 295 K resulting in O(1s) and C(1s) features identical to those observed at 295 K but after exposure at lower temperatures and low pressure ($\sim 10^{-6}$ Torr). The reaction showed all the characteristics associated with the participation of a

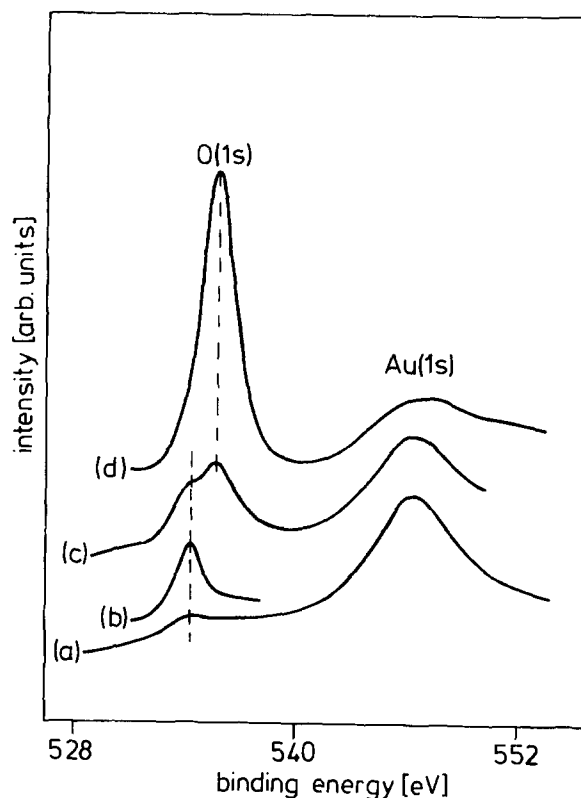


Fig. 13. O(1s) and Au(4s) photoelectron spectra of $\text{CO}_2/\text{Au}(\text{poly})$ [69] at 77 K. Various CO_2 dosages have been applied at: (a) equilibrium and 2×10^{-9} Torr; (b) equilibrium and $\approx 10^{-8}$ Torr; (c) 100 L; (d) 12000 L.

precursor state and the Freund–Messmer mechanism [34] was invoked where the dimer ($\text{CO}_2^- \cdots \text{CO}_2$) present at 80 K but only at “high pressures” at 295 K, was the key feature of the mechanism.

The high reactivity involving low energy pathways leading to the dissociative chemisorption of CO_2 was surprising. Was this unique to magnesium and aluminium or was the low energy pathway a consequence of CO_2 reactivity being induced by X-rays or photoelectrons? Clarification of this was sought through studies of both gold and bismuth surfaces [91].

At a $\text{Bi}(0001)$ surface CO_2 adsorbs at 80 K giving rise to O(1s) and C(1s) peaks at binding energies of 535 and 291.5 eV respectively. The corresponding loss features are at 670, 1360 and 2370 cm^{-1} . These are assigned to the bending mode $\delta(\text{OCO})$, and the symmetric stretching mode $\nu_s(\text{OCO})$ which is in Fermi resonance with the first overtone of $\nu_a(\text{OCO})$ respectively. All these loss features have direct counterparts in vibrational studies of gaseous carbon dioxide. Clearly at 80 K the adsorbed carbon dioxide is essentially unperturbed compared with the gas phase – in other words very weakly adsorbed. On warming to 295 K desorption occurs to leave an atomically clean $\text{Bi}(0001)$ surface. There is no evidence for any chemical reactivity induced by either X-ray or photoelectrons. Very similar results were reported for $\text{Au}(100)$ surfaces indicating that processes analogous to the Freund–Messmer dimer reaction, but where electron attachment to physically adsorbed CO_2 might be photon induced, did not occur. However, the presence of sodium at the $\text{Au}(100)$ surface led to high reactivity with carbonate formation occurring readily (see Section 7).

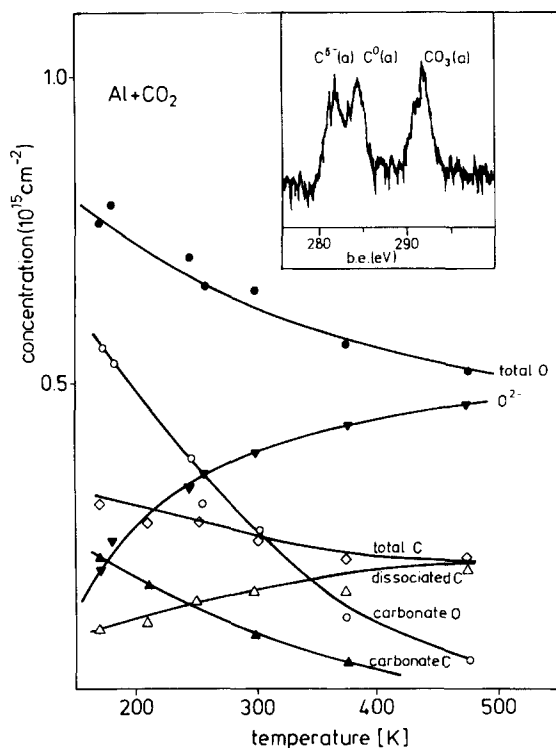


Fig. 14. Quantitative analysis of C(1s) and O(1s) photoelectron spectra of a $\text{CO}_2/\text{Al}(\text{poly})$ [89,90] adsorbate at various surface temperatures. A C(1s) photoelectron spectrum at $T = 295 \text{ K}$ is given as an example in the inset.

4.2. Interaction of CO_2 with transition metal single crystals

The interaction between CO_2 and metal single crystals has been studied extensively recently. Table 2 summarises much of these results [39,64,74–76,81,87–164]. Following our discussion on the possible pathways involved in the surface chemistry of CO_2 we consider the various key species involved: physisorbed CO_2 ; chemisorbed $\text{CO}_2^{\delta-}$; CO_2 dissociation, carbonate, and oxalate formation. Physisorption is found in almost all cases when the temperature approaches 80 K. The chemisorbed species are only observed under very specific conditions: the surfaces have to be either atomically rough, contain a high defect density in order to stabilize the chemisorbed species, or are alkali metal modified surfaces. As will be discussed in detail below, the chemisorbed species is connected with the formation of $\text{CO}_2^{\delta-}$, the anionic molecule, which involves charge transfer from the metal to the molecule. Therefore, the work function of the system should play an important role in the sense that relatively open surfaces as well as steps exhibit relatively low work functions, and thus favour electron transfer. The observation of $\text{CO}_2^{\delta-}$ in certain cases, of course, does not exclude its intermediate formation in other cases, where only reaction products, i.e. $\text{CO} + \text{O}$ dissociation products and/or carbonate formation is observed. It is as yet not clear which factors control the reaction pathways followed but that various low energy pathways are available is beyond doubt. We discuss in detail CO_2 adsorption on Ni(110), in order to illustrate how the application of various surface sensitive methods can provide a detailed picture of the chemistry involved.

Table 2
CO₂ adsorbates on metal surfaces

	CO ₂ (phys.)	CO ₂ ⁻ (chem.)	Dissociation	Carbonate	Oxalate	Ref.
Silver						
Ag(110)	x					[92–94]
Ag(110) + O	x			x		[86,95]
Ag(powder) + O	x			x		[96–98]
Aluminium						
Al(foil)	x		x	x		[89,90,99,100]
Al(100) + Na	x			x	x	[101,102]
Gold						
Au(poly)	x					[91]
Au(100)	x					[99,100]
Au(poly) + Na	x			x		[91]
Bismuth						
Bi(0001)	x	x	x	x		[91]
Copper						
Cu(film)	x	x				[103,104]
Cu(poly)	x	x	x			[105,106]
Cu(powder)	x		x			[107]
Cu(100)	x		at high p			[108–110]
Cu(100)	x	x in reaction				[99,100]
Cu(110)						[111,112]
Cu(111)						[113]
Cu(211)	x	x	x	x		[106]
Cu(311)	x	x(?)	x			[114]
Cu(332)	x	x(?)	x			[115]
Cu(110) + O	x					[116]
Cu(110) + O	x	x				[117]
Cu(211) oxidized	x	x				[106]
Cu(110) + Cs	x		x	x		[111]
Cu(110) + Cs	x	x	x	x		[117,118]
Cu(100) + K	x		x	x		[119]
Cu(110) + K	x	x	x	x		[120]
Cu(110) + K	x	x	x	x	x	[112]
Iron						
Fe(film)						[121,122]
Fe(film, annealed)	x	x				[74,75,121,122]
Fe(film) + O	x					[123]
Fe(100)	x	x				[124]
Fe(110)	x					[74,75,121,122]
Fe(110)	x		x			[125]
Fe(111)	x	x	x			[75,76,121,122]
Fe(100) + K	x	x	x	x	x	[126]
Fe(110) + K	x	x	x	x	x	[127,128]
Iridium						
Ir(110)(1 × 2)	x					[129,131]

Table 2 (continued)

	CO ₂ (phys.)	CO ₂ ⁻ (chem.)	Dissociation	Carbonate	Oxalate	Ref.
Magnesium						
Mg(000 1)	x		x	x		[88]
Mg(000 1)	x	x	x	x		[106]
Nickel						
Ni(1 0 0)	x		x			[131,132]
Ni(1 1 0)	x	x	x			[39,81,131,133]
Ni(1 1 1)	x					[134]
Ni(1 0 0) + O	x			x		[135,136]
Ni(1 1 0) + O	x			x		[39]
Ni(1 1 1) oxidized	x	x	x	x		[137]
Palladium						
Pd(1 0 0)	x					[138]
Pd(1 1 1)	x					[139–142]
Pd(1 0 0) + K	x	x	x	x		[143]
Pd(1 1 1) + Na, $\theta < 0.25$	x		x			[139–141]
Pd(1 1 1) + Na, $\theta > 0.25$	x			x		[139–141]
Pd(1 1 1) + K	x	x		x		[142]
Pd(1 1 1) + K	x	x	x			[144]
Platinum						
Pt(foil)	x					[145,146]
Pt(FEM-tip)	x					[147]
Pt(1 1 1)	x					[148–150]
Pt(1 1 1) + K	x	x		x		[150,151]
Rhenium						
Re(000 1)	x	x	x			[75,152–154]
Re(000 1) + Cu	x		x			[153]
Rhodium						
Rh(film)	x					[64]
Rh(poly)	x					[155]
Rh(Alumina-supp.)	x					[156]
Rh(FEM-tip)	x	x				[147]
Rh/B-impurities	x	x				[157,158]
Rh(1 1 1)	x					[152,153,157,158]
Rh(1 1 1) + K	x	x	x	x		[159–163]
Ruthenium						
Ru(00 1) + K	x	x	x	x	x	[164]

Work function measurements are shown in Fig. 15 [39]. At low coverage for CO₂/Ni(1 1 0), but also for other systems such as CO₂/Fe(1 1 1), an increase in the work function is observed. Depending on the substrate temperature, the work function passes through a maximum when going to higher coverages. If the surface temperature is high enough, the work function only reaches

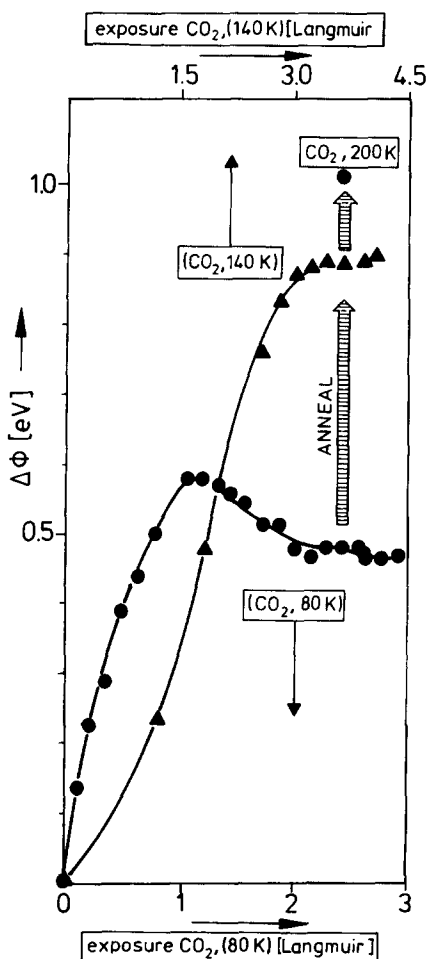


Fig. 15. Work function changes after exposing a Ni(110) surface to various dosages of CO₂ at different surface temperatures [39]. A single data point for $T = 200$ K is also included.

a saturation value and does not decrease. This observation indicates that there are likely to be two different species involved, one causing the work function increase and a second one, which is adsorbed at higher exposure, leading to a work function decrease. Photoemission may be used [12,13] to show that the second species present only at lower temperature is physisorbed CO₂ which exhibits a photoelectron spectrum basically identical to the one found for condensed multilayers of CO₂ [36,37]. The species giving rise to a work function increase may be identified as CO₂⁻ on the basis of vibrational spectroscopy. Fig. 16 shows a set of HREEL spectra as a function of surface temperature. At lowest temperature and the chosen exposure of 1 L both species are present on the surface. The spectral features are marked accordingly. Table 3 collects the frequencies for this and a number of other CO₂ adsorbate systems. The frequencies of the physisorbed CO₂ species are not listed because they agree to a large extent with gaseous CO₂ (see Fig. 4).

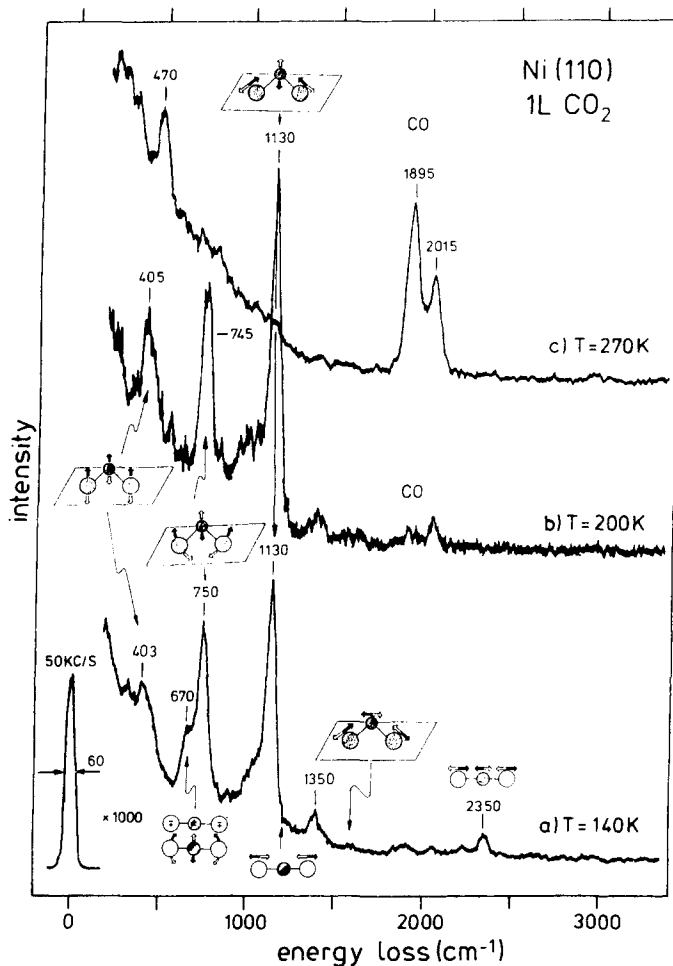


Fig. 16. Electron energy loss spectra of CO_2 adsorbed (1L) on Ni(110) at increasing surface temperature [39]. The assignment of the bands is schematically indicated in the figure and discussed in the text.

Table 3
Vibrational frequencies (cm^{-1}) of CO_2 chemisorbates

System	$\nu_{\text{M-mol}}$	δ	ν_{sym}	ν_{as}	$\nu_{\text{C-H}}$	Ref.
$\text{CO}_2/\text{Ni}(110)$	410	750	1130/1390	1620		[39,133]
$\text{CO}_2/\text{Re}(0001)$		(650)	1230	1625		[152–154]
$\text{CO}_2/\text{Fe}(111)$	401	800	1064/1160	1360/1600		[54,76]
$\text{CO}_2/\text{Fe}(100)$			1232	1634		[124]
$\text{CO}_2/\text{Na} + \text{Pd}(111)$	282	744	1210	1530		[139–141]
$\text{CO}_2/\text{K} + \text{Pt}(111)$		820	1340	1600		[148–150]
LiCO_2		750	1330	1569		[165]
$\text{HCOO}^-/\text{Ni}(110)$	403	727	1353		(2904)	[81]

Angle resolved photoelectron spectroscopy suggests [39] that for CO_2 physisorbed at Ni(110) the molecule is present with a strongly inclined geometry the axis almost parallel to the surface. This is also in line with the EELS observation of a low intensity symmetric CO_2 stretching band as compared with the bending vibration. In contrast to this the analysis of HREELS intensities for physisorbed CO_2 on Fe(111) suggests that CO_2 is adsorbed in a vertical geometry [76]. The frequencies of the chemisorbed species on Ni(110) are considerably different from the physisorbed ones. The observed changes are in line with the formation of adsorbed CO_2^- as judged by comparing the frequencies in Fig. 4 and Table 3. The band near 400 cm^{-1} for the unmodified surface is assigned to the frustrated molecule–surface vibration. The others are due to internal modes. Their frequencies vary for the different systems. Unfortunately, for none of the systems the adsorption site is known, indirect arguments being used to support a particular site. Comparison with the modes of coordination in transition metal complexes is however useful. As alluded to above, ideally, pure carbon or pure oxygen coordination leads to sites with C_{2v} symmetry as indicated in Fig. 17. Mixed carbon/oxygen coordination leads to sites with C_s symmetry (see Fig. 17) but depending on the surface geometry a clear distinction may not be possible. If we assume the idealized situation, then the vibrational modes schematically shown in Fig. 17 may be classified as given according to their irreducible representations. Under these circumstances the totally symmetric b_2 mode would not be dipole active as long as the surface site has C_{2v} symmetry. In C_s symmetry all modes are active.

Angle dependent HREELS measurements should in principle allow a distinction to be made between the symmetries. Unfortunately, only in a very few cases have off-specular measurements been reported, with data for the $\text{CO}_2/\text{Fe}(111)$ system [76] being the most complete. Similar data are

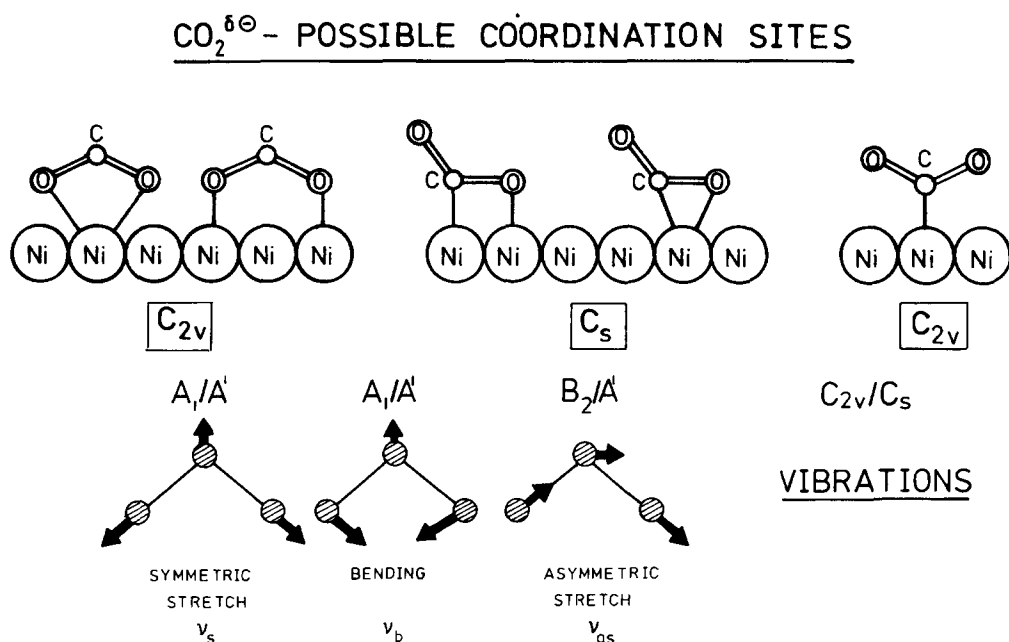


Fig. 17. Schematic representation of the stretching and bending vibrations in bent CO_2^- for the three types of CO_2^- coordination (see text). The irreducible representations of the vibrations are given for the sites of C_{2v} and C_s symmetries.

available for $\text{CO}_2/\text{Ni}(110)$ [39], both sets of data indicating that a band at or slightly above 1600 cm^{-1} is only observable in off-specular scattering. Since this is the energy range where the asymmetric stretch of CO_2^- is expected when it is bound in C_{2v} symmetry a tentative site assignment may therefore be possible. However, in the case of $\text{CO}_2/\text{Fe}(111)$ two CO_2 surface species are present, which makes a definite analysis difficult. In the case of $\text{CO}_2/\text{Ni}(110)$ the situation is less complicated in that there is only one species, $\text{CO}_2^{\delta-}$, present. The band at 1390 cm^{-1} with $\text{Ni}(110)$ is due probably to the high reactivity of $\text{CO}_2^{\delta-}$. There are two possibilities. First is the formation of carbonate via the reaction of surface oxygen stemming from CO_2 with coadsorbed molecular CO_2 . However, in this case, other intense bands are expected [58] which are not observed in the spectrum. This renders this possibility rather unlikely. Secondly there is the possible formation of surface formate from CO_2 and inadvertent hydrogen which may be on the surface (see below). Table 3 collects the observed vibrational frequencies of this species for comparison. HCOO^- is known to adsorb within a local C_{2v} symmetry [81] with pure oxygen coordination because the carbon is hydrogen bound and thus blocked as coordination site. Its symmetric stretching mode is located near 1350 cm^{-1} , i.e. in the range of the extra feature. Interestingly, all other bands are very close to the CO_2^- frequencies which is not too surprising because the symmetric C–H motion will couple most effectively to the symmetric O–CO mode. Since it may be shown that CO_2^- readily reacts with coadsorbed hydrogen to form formate on $\text{Ni}(110)$ [80] (see below) this explanation for the observation of the feature in the spectrum is likely. On the other hand, the similarity of the formate frequencies with the CO_2^- frequencies and the absence of the ν_{sym} in specular scattering geometry are both rather strong indications that CO_2 on $\text{Ni}(110)$ resides in a C_{2v} site. As mentioned above calculations [34] indicate that the energy difference between pure oxygen and mixed carbon–oxygen coordination is not very large. Therefore depending on the metal substrate and the sites provided by the surface, adsorbates with C_s and C_{2v} symmetry may be found simultaneously. It appears that $\text{Fe}(111)$ is such a case. Also, if the metal surface is modified, e.g. by coadsorption of an alkali metal, CO_2^- formation may be facilitated [8,91], but also reduced in adsorbate symmetry if CO_2 adsorbs near the coadsorbed atom [139–141]. The cases listed in Table 3 indicate the presence of the asymmetric stretch pointing towards a reduced symmetry of the adsorption complex.

To summarize at a $\text{Ni}(110)$ surface CO_2 chemisorbs in a bent geometry and of the different possible adsorption site symmetries the pure oxygen coordination with C_{2v} symmetry is most likely. The chemisorbed species is stable from below 100 K to about 150 K. Above 150 K the molecule is highly reactive. With atomically clean Ni, Fe, Rh and Re single crystal surfaces CO_2 dissociates into chemisorbed CO and oxygen. With $\text{Ni}(110)$ there is evidence (Fig. 16) for dissociation from the presence of strong CO losses and oxygen–surface vibrations. On other surfaces such as Pt, Pd, Os, and Ag, CO_2 does not appear to chemisorb although physisorption occurs (see Table 2). However, with these surfaces, reactions resulting in surface carbonate are observed frequently. The phenomena discussed so far have been observed using HREELS, however other spectroscopic methods such as XPS and Raman scattering do also provide a clear distinction between CO_2^- and CO_2 . Fig. 18 shows for the $\text{CO}_2/\text{Ni}(110)$ system C(1s) and O(1s) spectra [77]. The surface was exposed to CO_2 at 90 K and the two O(1s) peaks correspond to physisorbed and chemisorbed CO_2 . As expected for an anionic species considerable chemical shift towards lower binding energy is observed with both O(1s) and C(1s) ionizations. We discuss below the fact that the intensity ratio physisorbed/chemisorbed changes under the influence of photons due to light induced anion formation, but only mention the relative intensities between oxygen and carbon signals. Since for physisorbed CO_2

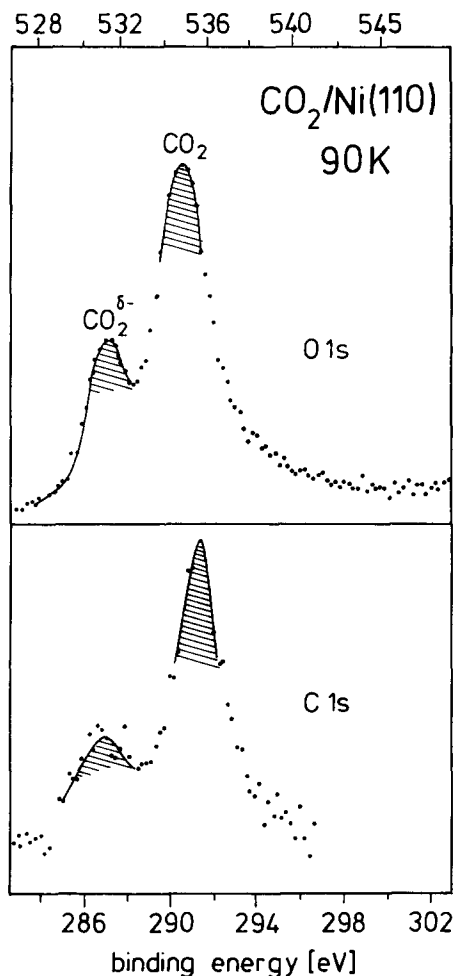


Fig. 18. C(1s) and O(1s) photoelectron spectra of CO₂ on Ni(110) at 90 K surface temperature [77].

the C:O stoichiometry is 1:2 and can be established experimentally we would anticipate for chemisorbed molecular species it will also be 1:2 which rules out an assignment of carbonate for this band, where the ratio would be C:O = 1:3. XPS therefore supports the HREELS assignments. Which factors influence the formation of chemisorbed CO₂? This is a question that is relevant to the dissociation of CO₂ in that it is likely to proceed via the intermediate state CO₂^{δ-}. The electronic configuration of the metal, its work function as a measure for the ease of electron transfer, and the influence of local geometry will all be relevant. In order to judge the importance of these parameters we consider some examples: All Ni surfaces physisorb CO₂ if the surface temperature is low enough (Table 2), however only the (110) surface chemisorbs CO₂. It is not very likely that this is due to structural effects, because formate generated by the chemisorption of HCOOH(g) bonds to both the (100) and the (110) surfaces. In this case, the relatively low work function of 4.5 eV could play a major role. This is about 0.5 eV lower than the work functions of the (100) and (111) surfaces. However, other surfaces with even lower work function (e.g. Cu) do not chemisorb CO₂ on any of the

low index surfaces (1 0 0), (1 1 0) and (1 1 1). The introduction of steps and defects however leads to CO_2 chemisorption as has been observed via surface enhanced Raman scattering by Akeman and Otto [103,104]. These authors report clear evidence for $\text{CO}_2^{\delta-}$ in their vibrational spectra. Further evidence for the influence of steps and structural defects on CO_2 chemisorption has been reported by Wedler and his group [74]. They showed in an interesting study of Fe(110), Fe(111) and polycrystalline films that the more open (1 1 1) surface does, indeed, lead to CO_2 chemisorption. So do polycrystalline iron films. Dwyer et al. showed later that Fe(100) also chemisorbs CO_2 [124]. Also relevant are the CO_2^- ion scattering data observed with various surfaces by Heiland, e.g. [134,144], where the CO_2^- ion is formed in the scattering process. This is clearly related to the charge-transfer ability of the surface.

In conclusion it is clear that with metal surfaces whether physisorbed CO_2 becomes chemisorbed depends on the metal, its work function, and on structural parameters including the presence of defects. The part the metal plays in this process becomes more obvious, when we consider whether or not dissociative chemisorption of CO_2 occurs leading to CO(a) and O(1a). Carbon monoxide and oxygen adsorption energies vary extensively with the metal and Fig. 19 shows a thermodynamic cycle, collecting all relevant energies in going from separated metal and CO_2 to CO and oxygen chemisorbed to the metal. Of course, independent of the metal the cleavage of one C–O bond in CO_2 requires 5.45 eV and if we now choose Ni as an example, 9.0 eV are needed to take an electron out of the metal ($\phi_{\text{Ni}} \approx 5.2$ eV), transfer the electron to CO_2 (0.6 eV), and then dissociate the CO_2^- formed. However, 9.54 eV are gained in the chemisorption of O^- and CO to the Ni surface. Therefore, there is an overall gain of 0.4 eV in the process of CO_2 dissociation at nickel surfaces within the simplified cycle. The process would on these arguments be expected to be highly metal specific and this is indeed the case.

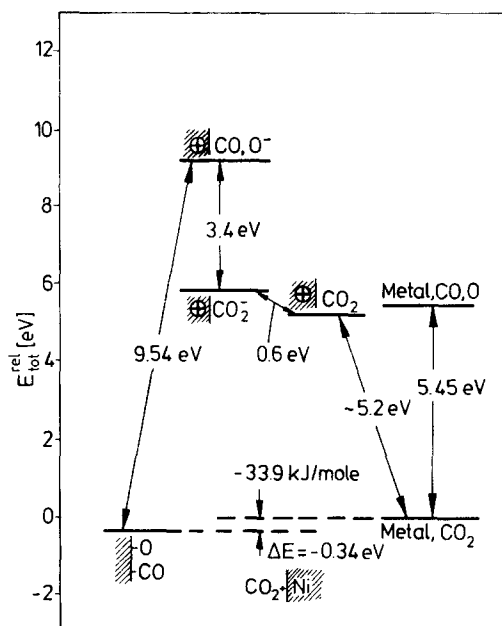


Fig. 19. Energy cycle for CO_2 dissociation into adsorbed CO and oxygen on a Ni surface. Energies are given in eV [34].

4.3. Adsorption of CO₂ at copper surfaces

Interest in the chemistry of carbon dioxide at copper was partly stimulated by the implications of the discovery made by the catalysis group of Imperial Chemical Industries that CO₂ is the main source of “carbon” in the synthesis of methanol using H₂–CO–CO₂ mixtures and their copper–zinc oxide catalyst [107]. The report of this discovery also coincided with publications relating to the reactive chemisorption of CO₂ at magnesium and aluminium surfaces [88–90,99,100]. We, therefore, turned our attention to the copper–CO₂ system [106]. It is also relevant to mention that just prior to this there had been considerable discussion as to whether or not CO₂ was dissociatively chemisorbed at rhodium surfaces [166,167], the possible role of surface structure in the dissociative chemisorption of CO₂ at Fe(1 1 0), Fe(1 1 1) and stepped Fe(1 1 0) surfaces [74], of alkali metal promotion in the reactivity of CO₂ at rhodium and palladium surfaces [138,143] and of alkali modified aluminium surfaces [101,102]. Although copper did not fit readily into the reactivity pattern associated with other transition metals, it had been shown to exhibit high reactivity (low energy pathway) for the dissociative chemisorption of nitric oxide and consequent formation of N₂O(g) and surface oxide [168]. In this case the thermodynamic driving force was surface oxide formation and the kinetics were clearly favourable in that N₂O formation occurred even at 80 K. The issue that intrigued us was whether CO₂ chemisorption at copper might exhibit analogous behaviour to that of nitric oxide and also of CO₂ with the sp-metals magnesium and aluminium [89,90]. Alternatively it might show characteristics closer to the weak chemisorption observed with CO at copper surfaces. Mitigating against the possibility of reactive chemisorption with copper, and resulting in surface carbonate and oxide formation, was the smaller inherent thermodynamic driving force compared with both magnesium and aluminium. Three different copper surfaces have been investigated; Cu(1 0 0), Cu(2 1 1) and Cu(pc). At polycrystalline copper surfaces, Cu(pc), together with physical adsorption at 80 K, there is evidence for an ionic form CO₂^{δ-} (a); these two species are characterized by C(1s) binding energies of 292 and 289 eV, respectively (Fig. 20). Very similar data were reported for a Cu(2 1 1)–O surface with evidence for CO₂(a) and CO₂^{δ-}(a) species characterized by C(1s) and O(1s) peaks at 293 and 533 eV for CO₂(a) and 289 and 531.5 eV for CO₂^{δ-} at low temperature (130 K). No carbon species were detected by XPS on warming the adlayer to 295 K [106].

At the intrinsically less reactive Cu(1 0 0) surface it was established that after characterizing with XPS, the physically adsorbed layer at 80 K, the adlayer was warmed to 160 K; XPS and EELS then established that a CO₂^{δ-}(a) species was present with a C(1s) peak at 289 eV and loss features at 340, 800 and 1500 cm⁻¹. A Cu(1 0 0) surface exposed to CO₂(g) at 80 K, but not characterized by either XPS or HREELS at this temperature, revealed no XPS evidence for any carbon dioxide species after warming the physically adsorbed layer to 130 K. This is positive evidence for the role of photons/electrons in CO₂ activation at copper surfaces. Extensive studies [169] using carefully purified CO₂ have confirmed this and established that traces of oxygen at the parts per million level (or less) can provide a highly efficient route to surface carbonate.

Although there is therefore unambiguous experimental evidence for the formation of anionic CO₂^{δ-}(a) species at copper surfaces the relative contributions of X-rays, photoelectrons, surface oxygen and surface structure to the activation of CO₂ at low temperatures is less clear. That anionic-like CO₂ species are favoured when alkali metal atoms (Cs) are present is unambiguous (see Section 7), furthermore when CO₂ is coadsorbed with molecules which are unreactive at copper

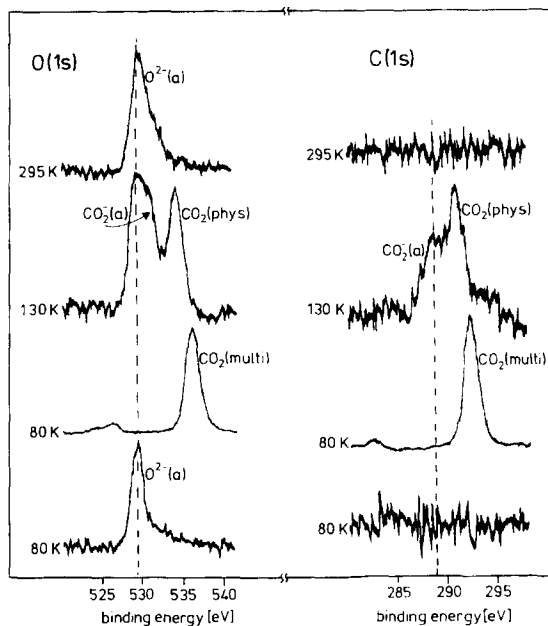


Fig. 20. O(1s) and C(1s) photoelectron spectra of an oxygen pre-dosed (50 L O₂) Cu(211) surface (lowest trace) exposed to 100 L CO₂ at 80 K (second), and then subsequently heated to 130 K and 295 K (upper traces) [106].

surfaces (e.g. NH₃) low energy pathways are available to reaction products (such as carbamate [170], Section 6). The consensus is that it is not too difficult to tip the energetics in favour of CO₂ reactive chemisorption at copper surfaces.

Campbell and Ernst [171] considered the elementary steps in the forward and reverse water gas-shift reaction $\text{CO} + \text{H}_2\text{O} \rightarrow \text{CO}_2 + \text{H}_2$. The dissociation of CO₂ occurs with a probability estimated to be about 10^{-9} per collision at 537 K at a clean Cu(1 1 0) surface. In the presence of chemisorbed oxygen the probability is greater, also the presence of H₂ is suggested to assist dissociative chemisorption and surface reconstruction is a postulated mechanism for this.

5. Chemisorption of CO₂ at oxide surfaces

Spectral identification of carbonate and carboxylate on powder surfaces has played a major role in the study of CO oxidation on oxide surfaces and there is a full, well documented literature on this subject [58,60]. We refer to this literature for further details and concentrate here on the study of CO₂ interaction with single crystal surfaces. Table 4 contains a collection of results for a variety of substrates [172–199]. With all substrates a physisorbed layer is formed at low temperatures. Heidberg and his group [177] have performed detailed studies of CO₂ adsorbates physisorbed on MgO. The molecules form ordered structures which have been characterized by LEED and FTIR spectroscopy. The structures may be compared with the studies of CO₂ on NaCl, also performed by Heidberg's group [200–205], and also by Ewing and coworkers [206]. In general chemisorption leads to the formation of carbonate. Only with ZnO was the formation of CO₂⁻ reported, i.e.

Table 4

	CO ₂ (phys.)	CO ₂ ⁻ (chem.)	Dissociation	Carbonate	Oxalate	Ref.
Barium oxide						
BaO(poly)	x			x		[171,172]
Calcium oxide						
CaO(100)	x			x		[173]
Chromium oxide						
Cr ₂ O ₃ (111)	x			x		[174]
Manganese oxide						
MnO(100)	x					[175]
Magnesium oxide						
MgO(100)	x					[173,176–179]
MgO(100)	x			x		[180,181]
MgO("111")						[181]
Sodium oxide						
Na ₂ O("100")	x			x		[182]
Na ₂ O("110")						[182]
Nickel oxide						
NiO(100)	x					[183]
Titanium dioxide						
TiO ₂ (110)	x			x		[184,185]
Zinc oxide						
ZnO	x but photo-r					[186]
ZnO(10 $\bar{1}$ 0)	x	x		x		[184,187–194]
ZnO(10 $\bar{1}$ 0)	x			x		[195]
ZnO(000 $\bar{1}$)						[196]
ZnO(000 $\bar{1}$)	x			x		[191]
ZnO(0001)	x	x				[191,197–199]
ZnO(40 $\bar{4}$ 1)	x					[192,193]
ZnO(50 $\bar{5}$ 1)	x					[192,193]

carboxylate structures [185,189–191]. Fig. 21 shows a schematic representation of the conclusions drawn, indicating carboxylate structures formed via coordination of a bent CO₂^{δ-} molecule to a metal centre. Carbonate structures may also be formed via coordination of a CO₂^{δ-} towards an oxygen atom. Although this configuration will result in monodentate carbonates it has not as yet been verified by vibrational spectroscopy. For CO₂ adsorption on Cr₂O₃(111) Kühlenbeck et al. [174] have observed the formation of a carbonate at low temperatures. Fig. 22 shows a correlation of the frequencies found in this study with the results shown in Fig. 8. From this it is clear that the frequencies are closer to those associated with a bidentate coordination. NEXAFS data [174] for the same system indicate the CO₃ plane is oriented perpendicular to the surface which would be consistent with a bidentate coordination. Stabilities of the carbonates on oxide surfaces have been investigated using thermal desorption spectroscopy and other techniques. At a Cr₂O₃(111) surface carbonate already forms at 100 K and it is stable to temperatures above room temperature [174,175]

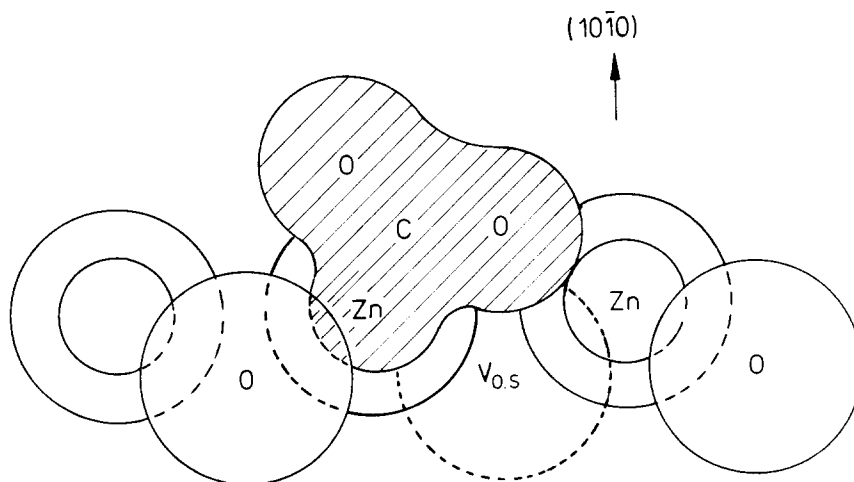


Fig. 21. Schematic representation of the structure of a CO₂ adsorbate on a ZnO surface as proposed by Göpel et al. [185,189-191].

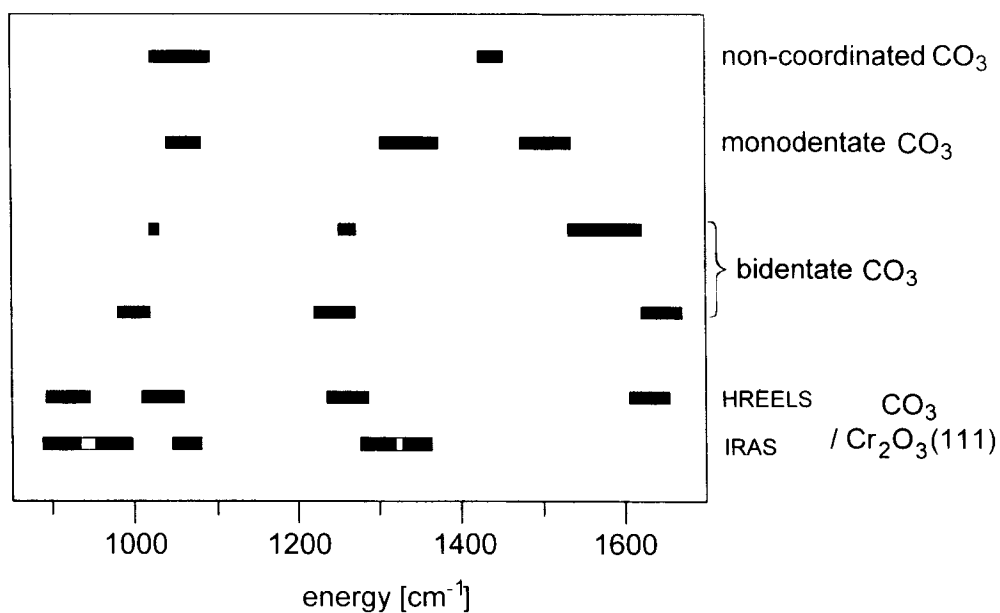


Fig. 22. Correlation diagram of the carbonate vibrational bands observed after dosing a Cr₂O₃(000 1) face to saturation (80 K) with some of the data shown in Fig. 8 [174,175].

in Table 4. As mentioned above, CO₂ does not strongly interact with non-polar (100) surfaces of rock-salt type oxides like MgO and NiO. Tanabe et al. [207] have studied the basic properties of the oxides



and found the order accordingly, where by basicity is meant the ability of the surface to donate charge to the adsorbed molecule. In order to judge this result which was gained on powder samples, it is important to exclude the influence of defects by studying single crystal surfaces. This has not yet been studied in detail but Pacchioni et al. [173] have theoretically analysed the situation by comparing MgO and CaO with respect to CO₂ and SO₂ adsorption. They find for CO₂ a weakly bound complex on MgO while a chemically bound carbonate is formed by coordination to an oxygen ion at the CaO surface.

The reason for the difference in reactivity may be understood from a theoretical study involving decomposing the interaction energy into electrostatic polarization and charge transfer contributions. The crucial factor is not chemical in origin, but can simply be explained in terms of the electrostatic stabilization of the surface anion. The O²⁻ ion at the surface is stabilized by the Madelung potential of the ionic crystal which is smaller with CaO than with MgO, thus leading to a higher basicity and reactivity of CaO. The smaller Madelung energy parallels the growth of the lattice constants. We may state that a regular site with CaO behaves like a defect site in MgO.

6. Reactions of CO₂ with coadsorbed species

As discussed in detail above the anionic form CO₂^{δ-} is stable at Ni(1 1 0) surfaces at temperatures up to 150 K. The adsorbed state represents a species with unsaturated valencies at the carbon atom and can be thought of as a radical anion. We may therefore envisage reactions of the CO₂⁻ with other atomic or molecular species either in the gas phase or as a surface species. A direct combination of two CO₂⁻ molecules is rather unlikely because the negative charge should lead to strong intermolecular coulombic repulsion (see however [102,103,209]). It is however feasible to consider a reaction between CO₂⁻ and neutral CO₂, i.e. within a solvation complex (see above). Fig. 10 schematically shows the reaction of CO₂ with hydrogen on Ni(1 1 0) to form formate [80].

In Fig. 23 a series of HREEL spectra is shown, the Ni(1 1 0) surface having been exposed first to 1 L CO₂ and subsequently to 0.1 L H₂. The reverse exposure does not lead to reaction. At 90 K the spectrum is very similar to the spectrum at the bottom of Fig. 16. If we increase the temperature, the physisorbed CO₂ desorbs and the intensity of the CO₂⁻ bands increase. Note that even at low temperature there is a small loss peak at about 1350 cm⁻¹. At 200 K, when CO₂⁻ would have dissociated at the clean surface, it is still present. However, the peak at 1350 cm⁻¹ has increased in intensity, also, at off specular scattering conditions a C–H vibration is observed close to 2900 cm⁻¹. A comparison with the vibrational frequencies given in Table 3 indicates that the new bands are due to adsorbed formate. Isotopic labelling experiments with D₂ prove that these are C–H vibrations. When we compare the vibrational frequencies in CO₂⁻ and formate it is mainly the symmetric stretching frequency that shifts by approximately 200 cm⁻¹ in formate, while the asymmetric stretch and the bending mode, as well as the molecule–surface vibration, are basically at the same frequency as in the case of CO₂⁻. There is, however, a considerable difference in the structure of the formate adsorbate as compared with the CO₂⁻ adsorbate, which we discussed above: NEXAFS data at the oxygen edge reveal the sharp π-resonances and the broad σ-resonances of both the CO₂⁻ and HCOO⁻ moieties. While for the case of CO₂⁻ there is no dependence on the azimuthal direction of

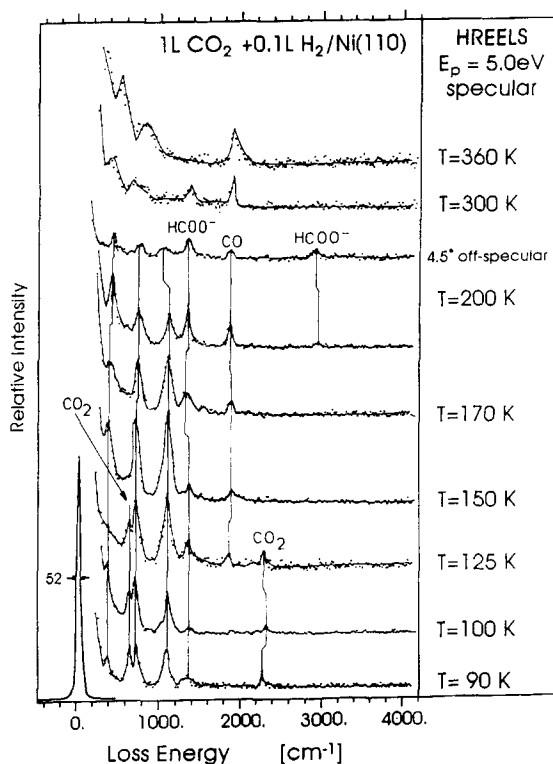


Fig. 23. Electron energy loss spectra of CO_2 and H_2 coadsorbed on a Ni(110) surface at 90 K. The surface has been subsequently heated to the temperatures indicated [80]. The spectra are recorded in specular scattering geometry unless indicated.

the incoming light with respect to the relative changes of intensities upon variation of the polar angle θ , the HCOO^- species does exhibit a pronounced azimuthal dependence. The observed behaviour of the polar angle variations are on one hand in line with the orientation of the molecular plane perpendicular to the surface plane for both species, and on the other hand in line with a preferential azimuthal orientation along the (110) of the formate species as opposed to a random orientation of the CO_2^- species. It would be interesting to understand this difference observed. In how far this structural flexibility has any relevance for the reactivity of CO_2^- towards coadsorbed species is not clear at present.

The formation of the surface formate species from CO_2^- and hydrogen can also be followed by XPS; the C(1s) spectra taken at high resolution are shown in Fig. 24. At the top we find coadsorbed CO_2 and CO_2^- at low temperature. On increasing the temperature the physisorbed species desorbs, and there are some indications for the formation of $\text{CO}_2^{\delta-}$. It is thought that the broad features in the spectra overlapping the peaks are due to solvated CO_2^- i.e. aggregates between CO_2^- and neutral CO_2 in various quantities. At around 180 K the chemical shift indicates the formation of formate which at higher temperature eventually dissociates and CO remains on the surface. It is thus obvious from a series of measurements using a variety of different experimental methods that CO_2 can react with hydrogen to form formate at a Ni single crystal surface.

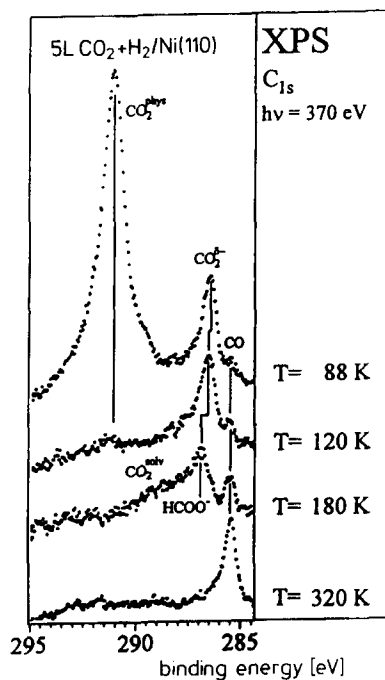


Fig. 24. C(1s) spectra recorded using monochromatized synchrotron radiation (Dragon beam line at NBL) after dosing a Ni(110) surface with CO₂ and H₂ at 80 K and subsequent heating [80].

This opened up the possibility of reacting CO₂ with other coadsorbed species. A particularly interesting reaction is that of CO₂^{δ-} and coadsorbed methyl groups to form acetate and involving the formation of a carbon–carbon bond. CH₃ species were generated by dissociative adsorption of CH₃I [209,210]. Fig. 25 shows the HREELS spectrum for an exposure of 2 L CH₃I to a Ni(110) surface at 95 K. The assignments of the bands are given by comparison with literature spectra [209,210]. When the adsorbate is heated, CH₃I dissociates with the formation of CH₃(a) and I(a) (Fig. 25) and reflected by the shift of the C–H stretching frequencies. These methyl groups are reactive as indicated by the TD spectra (Fig. 26). We observe not only the desorption of CH₃ and CH₄ but also of ethane leading to a sharp desorption signal with maximum around 135 K. If we preadsorb CH₃I (see Fig. 25), we do see the CO₂^{δ-} signals in the HREEL spectra (Fig. 25) attenuated without simultaneous desorption of CO₂. Concomitantly, we observe the formation of a carboxylic species, characterized by the vibrational frequencies, but it is very difficult at present to differentiate between formate and acetate formation. In order to differentiate between acetate and formate species we need to identify the C–C stretching vibration. However even for pure acetate adsorbates the C–C intensity is weak (see Fig. 25), which does not help. Isotopic labelling experiments and FTIR investigations for the same system are under way to shed more light onto this question. There is one hint for the formation of acetate species in the recorded TD spectra. At rather low temperatures, in the range where CO₂^{δ-} becomes unstable with respect to dissociation we observe a peak characteristic of CH₃CO (*m/q* = 43), the major fragment in the fragmentation pattern of CH₃COOH. This points

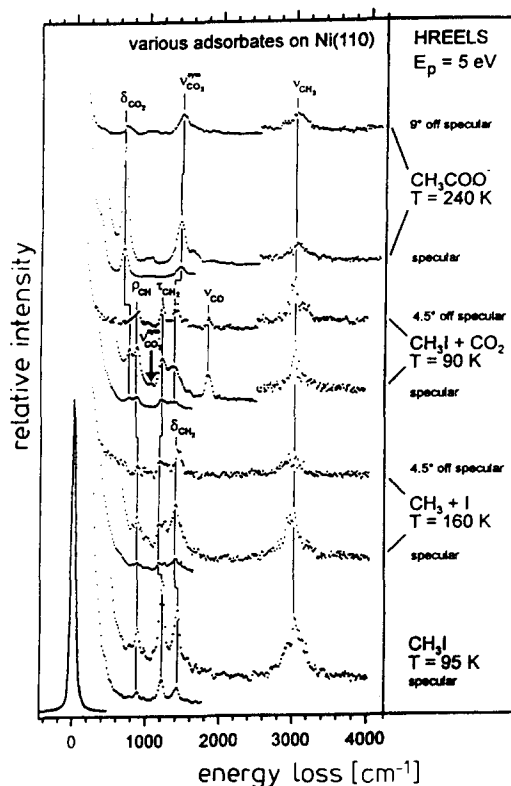


Fig. 25. Electron energy loss spectra of various co-adsorbates of CO_2 and CH_3I as well as of a pure CH_3I adsorbate at different temperatures and scattering conditions as indicated [209,210].

at least to the formation of a carbon–carbon bond but whether this bond is established between CO_2^- and CH_3 or CH_3 and CO is not clear at present. The TD spectra for CO_2 ($m/q = 44$) and HCOO ($m/q = 45$) are similar to those observed in formate adsorption.

An aspect of surface chemistry that has emerged only recently is that the reactivity of coadsorbed molecules cannot readily be predicted from the known chemistry of the molecules studied separately. This has been a particular feature of the chemistry observed when molecules are coadsorbed with dioxygen with evidence for the participation of oxygen transients established – with the metal determining which transient is likely to be significant [99]. Although CO_2 and NH_3 are relatively unreactive at a $\text{Cu}(100)$ surface and not adsorbed at 295 K, when coadsorbed a carbamate species is formed readily [170]. Ammonia is an effective electron donor and also when physically adsorbed lowers the work function of a surface. A relatively simple model for the chemistry observed when CO_2 and NH_3 are coadsorbed is that electron donation into the antibonding orbital of CO_2 leads to the reactive, bent anionic form $\text{CO}_2^{\delta-}$ with H-elimination from NH_3 giving $\text{NH}_2\text{-CO}_2(\text{a})$ [170]. The HREEL spectrum (Fig. 27) exhibits all the features expected of a surface carbamate with the core-level $\text{O}(1s)$, $\text{C}(1s)$ and $\text{N}(1s)$ spectra exhibiting the following binding energies 531.3, 289 and 400 eV, respectively. These binding energies are compatible with the functional groups CO_2 and

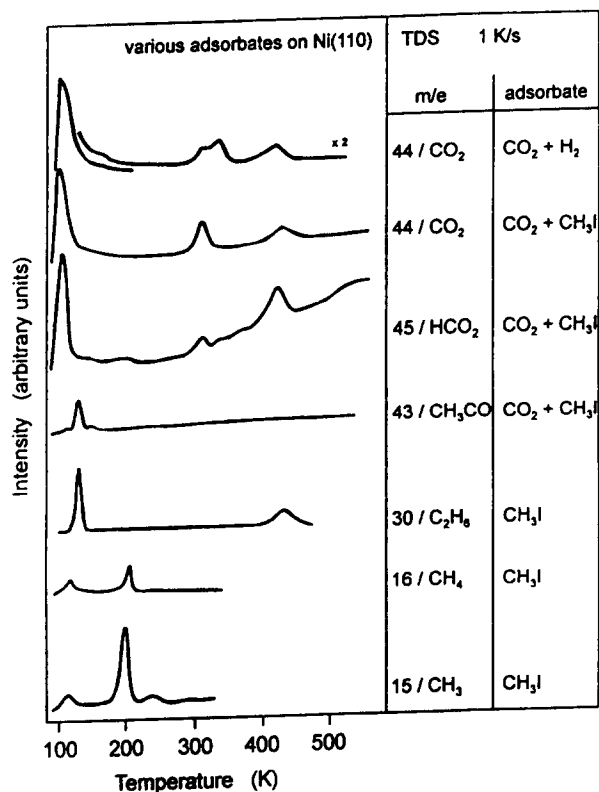
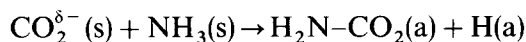
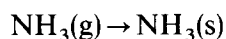
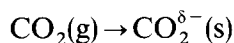


Fig. 26. Thermal desorption spectra of various adsorbates involving CO₂ and CH₃I for characteristic masses (*m/e*) as indicated [209,210].

NH₂ being present at the surface.



A further example of the chemical reactivity of CO₂ when coadsorbed is that a low energy pathway to surface formate has been revealed through the coadsorption of carbon dioxide with water at low temperatures at an Al(111) surface [208]. Both core-level and HREEL spectra indicate the presence of formate with a characteristic $\nu(\text{C}-\text{H})$ stretch at 2960 cm^{-1} and $\delta(\text{OCO})$ and $\nu(\text{OCO})$ losses at 840 and $1500\text{--}1600 \text{ cm}^{-1}$, respectively. The vibrational spectrum was shown to be indistinguishable from a model surface formate generated by the interaction of formic acid with Al(111).

The role of surface formate in methanol synthesis over copper catalysts – including single crystals of copper – has received much attention over the last decade. That surface formate can be generated

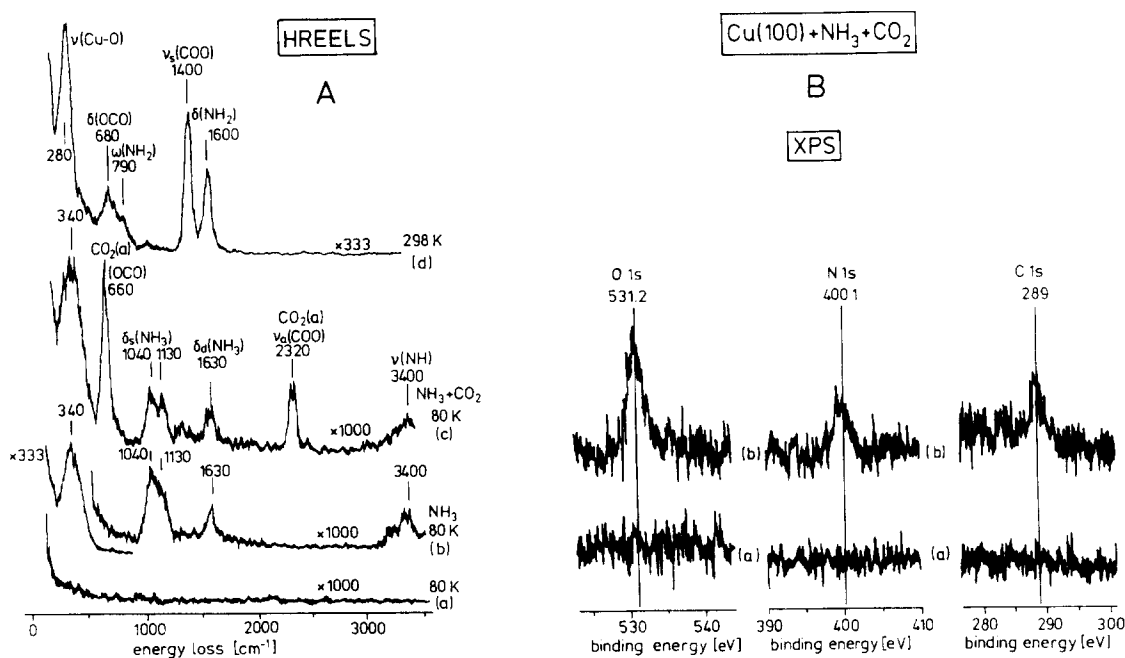


Fig. 27. (A) Electron energy loss spectra of Cu(100) exposed to ammonia and ammonia/ CO_2 coadsorbates [170]; (a) clean surface at 80 K; (b) $2 \times 10^{15} \text{ NH}_3 \text{ mol cm}^{-2}$ at 80 K; (c) exposure of (b) to 10 L CO_2 at 80 K; (d) exposure of (c) heated to room temperature. (B) C(1s), N(1s) and O(1s) photoelectron spectra of a Cu(100) (clean (a)) surface exposed to NH_3 and CO_2 at 80 K and subsequently warmed to room temperature (b); compare with (d) in Fig. 27 (A) [170].

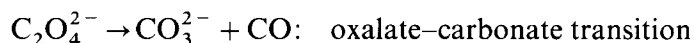
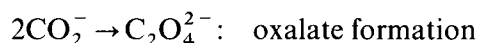
from hydrogen–carbon dioxide mixtures over copper is controversial in that Burch et al. see no evidence [211] for formate using FTIR in the case of a copper – zinc oxide catalyst while (for example) Taylor et al. [212] report spectroscopic evidence for surface formate at 2.3 bar pressure and 363 K with Cu(100). In post reaction analysis of the surface, these authors observed loss peaks in the HREEL spectra at about 800, 1300 and 2900 cm^{-1} and assigned to $\delta(\text{OCO})$, $\nu_s(\text{OCO})$ and $\nu(\text{C-H})$.

7. Alkali metal activation of CO_2 at metal surfaces

Alkali metal activation of adsorbates has been extensively studied over the last decade using surface sensitive spectroscopies; these studies were largely motivated by the need to understand their role as catalytic promoters, whether in ammonia synthesis or hydrocarbon chemistry [213]. The flurry of activity with relation to CO_2 chemistry started in 1986 with contributions from Berko and Solymosi [143] and Paul [101] and somewhat later by Solymosi and Bugyi [159] and Paul and Hoffmann [102]. More recently the experimental work, mainly HREELS, has been supplemented by theoretical studies of possible reaction pathways for CO_2 reactions [111].

There is unanimity in the view that alkali metal atoms, present at both transition and sp-metal surfaces, effect activation of an adsorbed CO_2 molecule [111]. What is less clear is the precise nature of the activated species and the reaction pathways followed subsequent to activation, although $\text{CO}_2^{\delta-}$ is a key intermediate.

Early studies with rhodium were controversial in that so-called “clean” surfaces showed variable activity in CO_2 dissociation, with Solymosi and Kiss [158] suggesting that boron impurities promoted CO_2 dissociation whereas atomically clean rhodium adsorbed CO_2 only in the molecular state. However, there was no ambiguity that a potassium modified rhodium surface led to the activation of the CO_2 molecule with desorption temperatures increasing from 230 K (clean surface) to 342 K ($\theta_K = 0.19$). The precise nature of the strongly adsorbed CO_2 species was less clear but charge transfer to an empty CO_2 π^* -orbital was a reasonable suggestion particularly since alkali metal atoms would be anticipated to lower the work function of the surface. The direct formation of the CO_2^- anion through interaction with a surface potassium atom was suggested; CO_2^- could subsequently generate surface carbonate or oxalate species which might decompose along various pathways:



Solymosi and Bugyi [159] postulated that the high temperature state giving rise to CO_2 desorption is probably a surface carbonate. Solymosi [8] returned recently to the rhodium–potassium system with the advantage of high resolution spectroscopy (HREELS) and reported losses at 2350, 1630, 1340, 840 and 640 cm^{-1} at 90 K for $\theta_K = 0.72$. Those at 840, 1360 and 1620 cm^{-1} they assigned to the CO_2^- (a) species. Other than the loss of features assigned to weakly (physically) adsorbed CO_2 at 2350 and 640 cm^{-1} – very little change was observed in the HREEL spectrum up to 500 K. Above this temperature the only loss feature present was at 1440 cm^{-1} and these authors suggest that an oxalate to carbonate transition occurs between 255 and 500 K.

Very recently CO_2 adsorption and reaction on potassium promoted Fe(1 1 0) has been studied using photoelectron spectroscopy and work function measurements [127,128]. The formation of carbonate and oxalate species is reported. Also the authors find an interesting potassium coverage dependent stability of carbonate. While for low coverages $0 < \theta_K < 0.2$ carbonate decomposes between 200 and 300 K the decomposition temperature is increased to 500 K for higher potassium coverages, i.e. $0.26 < \theta_K < 0.3$.

The reactivity of alkali promoted Cu(1 1 0) surfaces to carbon dioxide has been studied [113,117], Cs/Cu(1 1 0) in particular using a combination of XPS and HREELS (Fig. 28). At 80 K loss features were present at 295, 660, 1460 and 1660 cm^{-1} , with a shoulder at 700 cm^{-1} . On warming to 298 K, the intensities of the strong losses at 660, 1460 and 1660 cm^{-1} decrease rapidly and are replaced by intense losses at 1510 and 350 cm^{-1} and a weaker feature at 1060 cm^{-1} .

There are three loss features we associate with physically adsorbed CO_2 , 660 cm^{-1} (strong), 1300 cm^{-1} (weak), and 2350 cm^{-1} . Only the 660 cm^{-1} loss is observed at 80 K and this is lost rapidly on warming to 298 K, as also are the two relatively strong loss peaks at 1460 and 1660 cm^{-1} which

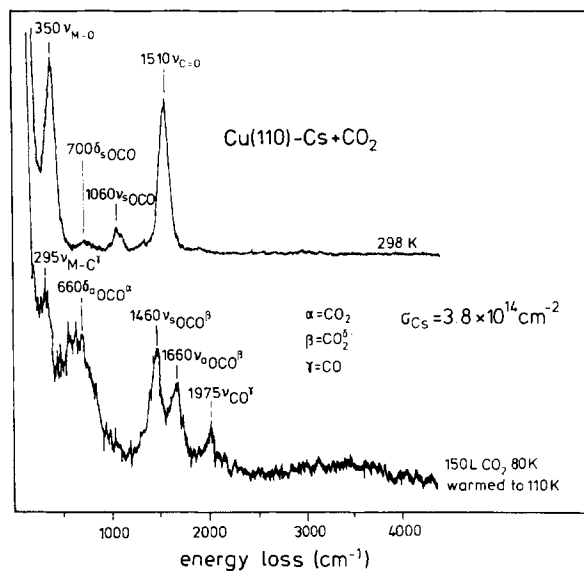


Fig. 28. Electron energy loss spectra of Cu(110) exposed to 3×10^{14} atoms cm^{-2} Cs and 150 L CO_2 at 80 K and subsequently heated to 110 K (lower trace) and room temperature (upper trace) [117].

are assigned to $\text{CO}_2^{\delta-}$ (a). These assignments are similar to those reported by Solymosi [8]. However at the Cu(110)–Cs surface (Fig. 28) the behaviour of these two loss features (1460 and 1660 cm^{-1} assigned to the symmetric and asymmetric stretches of $\text{CO}_2^{\delta-}$) differ markedly from the temperature dependence of the analogous features (1340 and 1620 cm^{-1}) observed by Solymosi at K-dosed Rh(111). In the latter case these losses were still present at 500 K whereas with the Cu(110)–Cs surface they had been replaced by a single intense carbonate feature at 1510 cm^{-1} ($\nu(\text{C}=\text{O})$). The XP spectra add support to this assignment [117].

An interesting aspect of the Cu(100)–Cs–O system is its high reactivity to carbon monoxide – the surface oxygen participating readily through a low energy pathway in the formation of $\text{CO}_2^{\delta-}$ at low temperatures and surface carbonate at higher temperatures [117]. In an attempt to understand the role of cesium we reported recently an XPS investigation of the chemisorption of oxygen by cesium multilayers at low temperatures [214]. Four oxygen states are delineated, with increasing oxygen exposure at 80 K with each state having associated with it a distinct O(1s) binding energy (Fig. 29). Initial interaction is dominated by the $\text{O}^{\delta-}$ species with an O(1s) binding energy of 531.5 eV but with increasing oxygen coverage this loses its identity and is replaced by two major oxygen states, O^{2-} and $\text{O}_2^{\delta-}$, with binding energies of 530.3 and 533.4 eV, respectively. The $\text{O}^{\delta-}$ species is highly reactive to carbon monoxide at 80 K generating the anionic state $\text{CO}_2^{\delta-}$ which has spectral features quite distinct from physisorbed carbon dioxide but identical with those observed when CO_2 interacts with atomically clean cesium (Fig. 30). Furthermore the $\text{O}^{\delta-}$ state is reactive to CO_2 at low temperatures to generate a surface carbonate whereas the $\text{CO}_2^{\delta-}$ surface species can be converted directly to carbonate by exposure to dioxygen at 80 K (Fig. 30).

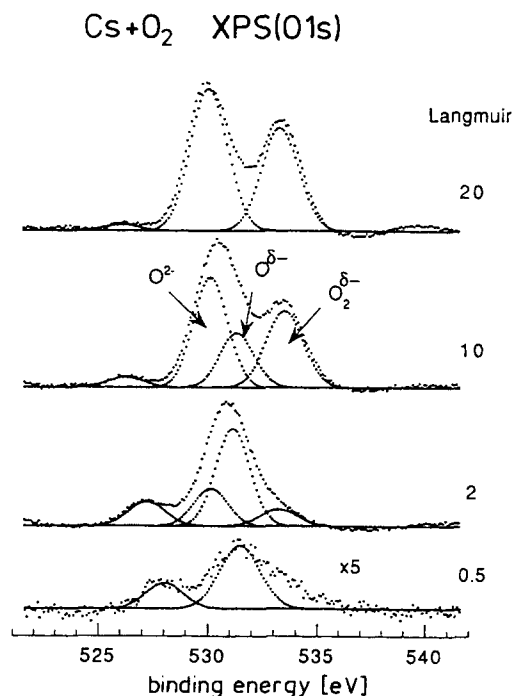
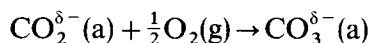
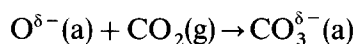


Fig. 29. O(1s) photoelectron spectra of a thick Cs film after various exposures to oxygen at 80 K [214].

These studies [214] have enabled us to isolate each of the individual steps involved in the formation of $\text{CO}_2^{\delta-}$ from carbon monoxide and the $\text{O}^{\delta-}$ state at Cs surfaces; the transformation of $\text{CO}_2^{\delta-}$ to carbonate by dioxygen and the reactivity of the $\text{O}^{\delta-}$ state to carbon dioxide to generate surface carbonate species. The overall chemistry involves



a sequence of individual inherently simple step-wise processes.

Although there had been indications from studies of alkali modified surfaces that the bent anionic adsorption state, $\text{CO}_2^-(\text{a})$, might participate in the surface chemistry of CO_2 , the first HREEL spectra were reported by Maynard and Moskovits [215]. These authors reported spectra (Fig. 31) for the adsorption of CO_2 on silver surfaces modified by cesium, potassium and lithium. Loss features were observed at 760, 1260 and 1600 cm^{-1} and assigned to the bending $\delta(\text{OCO})$ and symmetric stretch (ν_s) modes of $\text{CO}_2^-(\text{a})$ while that at 1600 cm^{-1} is the antisymmetric (ν_a) stretch of the CO_2^- ion. These compare with 1460 and 1660 cm^{-1} observed for CO_2 interaction with a Cu(1 1 0)-Cs surface (Fig. 28). There is also intensity at $\sim 700 \text{ cm}^{-1}$ which overlaps with a feature due to physisorbed CO_2 at 660 cm^{-1} (Fig. 28).

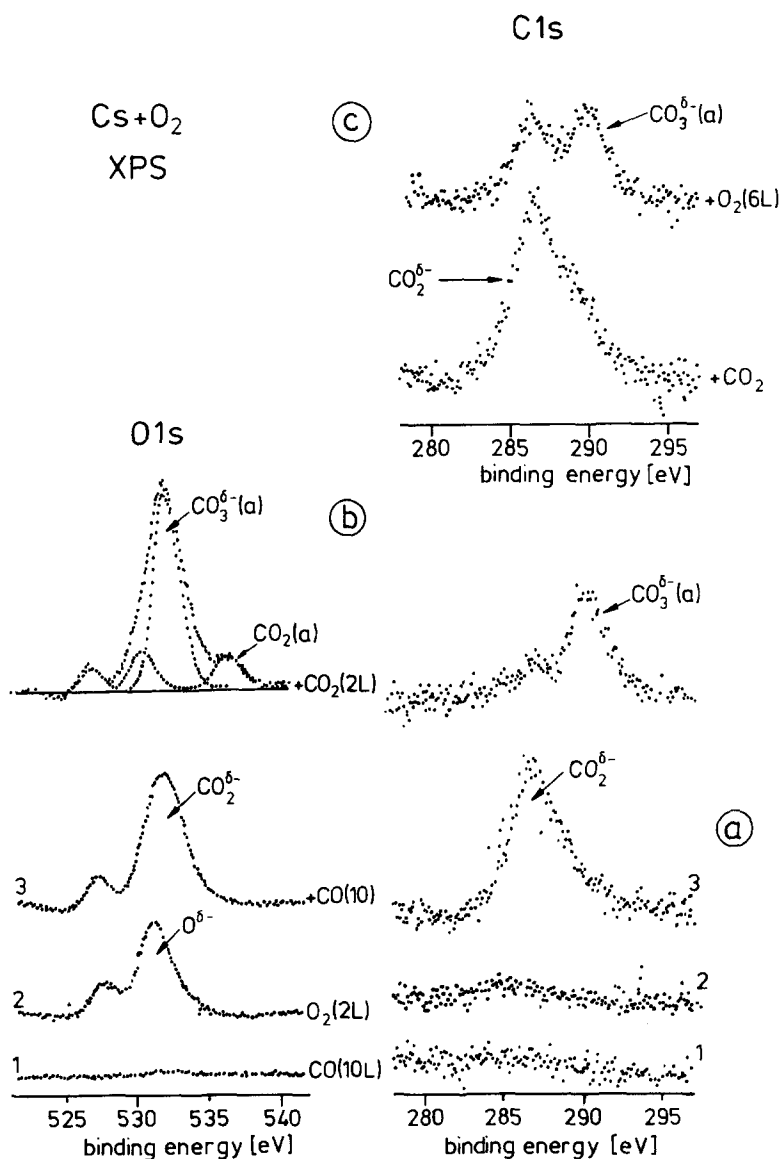


Fig. 30. (a) O(1s) and C(1s) spectra for Cs multilayers after: CO exposure at 80 K (spectrum 1) – there is no evidence for adsorption; exposure to oxygen at 80 K resulting in O^{δ-} formation (spectrum 2); exposure of O^{δ-}(a) to CO(g) at 80 K with formation of CO₂^{δ-} (spectrum 3) [214]. (b) O(1s) and C(1s) spectra after exposure of O^{δ-} species to CO₂ at 80 K; formation of CO₃^{δ-} species [214]. (c) Partial conversion of CO₂^{δ-} species to CO₃^{δ-} on exposure to O₂ at 80 K; C(1s) spectra [214].

8. Summary and conclusions

The surface chemistry of carbon dioxide received relatively little attention during the period 1960–1980 when at the same time carbon monoxide dominated the surface science literature. The lack of interest in carbon dioxide chemistry can be attributed to its thermodynamic stability but the

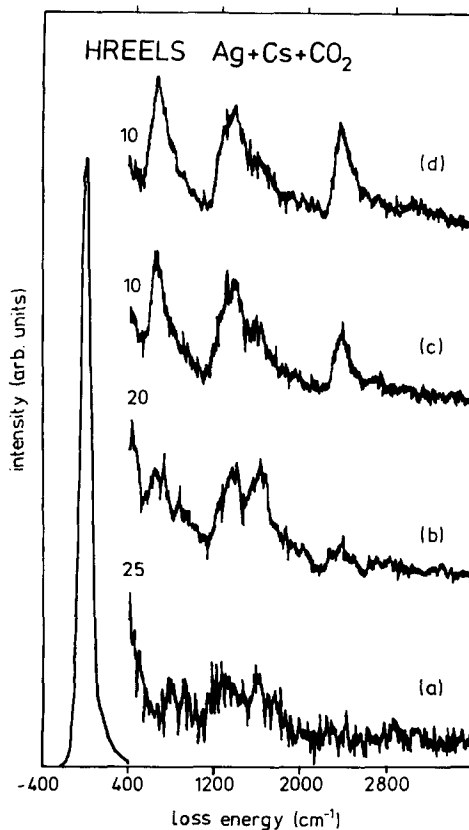


Fig. 31. Electronic energy loss spectra for a cesium modified silver surface after various exposures to CO_2 at low temperature: evidence for a $\text{CO}_2^{\delta-}$ species, (a) 1 L, (b) 2 L, (c) 4 L, (d) 7 L [215]. Note close similarity with assignments for the Cu(1 1 0)-Cs system [117] and Fig. 28.

realization that it was the key reactant in methanol synthesis in the early 1980s offered significant impetus to surface science studies. In this review we see how studies reported in the 1950s largely with metal powder and evaporated films provided some hints on its reactivity and infrared evidence for carboxylate structures involving a “bent” carbon dioxide molecule. The latter has been central to the understanding of the reactivity of carbon dioxide and the interpretation of vibrational and photoelectron spectra at single crystal metal surfaces over the last decade.

The formation of the bent anionic form of carbon dioxide has been addressed from a theoretical viewpoint with solvation of the $\text{CO}_2^{\delta-}$ species playing a significant role in its chemistry. The solvated species ($\text{CO}_2^{\delta-} \cdots \text{CO}_2$) is the essential precursor in the facile formation of such reaction products as carbon monoxide, carbonate and oxalate with spectroscopic (HREELS and XPS) evidence provided for each step in the reaction.

Electron transfer from the surface to form $\text{CO}_2^{\delta-}$ can be influenced by both the presence of alkali metals (such as cesium and potassium) and surface structure. There is little distinction that can be made between the chemical reactivity of transition and sp-metals but the presence of alkali metal

promoters confers high chemical reactivity in all cases. The particular reaction pathway chosen being dependent on the alkali metal coverage. The reactivity of oxidized multilayers of cesium provides evidence for specific oxygen states that are highly reactive to both CO and CO₂ to give CO₂^{δ-} and CO₃ respectively.

The coadsorption of CO₂ with other molecules – ammonia and methyl iodide for example – provides low energy pathways to products where again the bent CO₂^{δ-} anionic species is crucial to the mechanism. The challenge is now to design catalysts that can provide ways in which CO₂ can be utilized as a C1 feedstock with hydrocarbon – carbon dioxide reactions being one of the most interesting challenges.

Acknowledgements

We are grateful to our coworkers who have contributed to the work over the years. We would like to mention in particular: B. Bartos, J. Wambach, S. Wohlrab, D. Ehrlich, O. Seiferth, B. Dillmann, A.F. Carley, P.R. Davies and M.K. Rajumon. O. Seiferth has also helped us with establishing the tables which was particularly important.

Several agencies have supported our group: Deutsche Forschungsgemeinschaft, Bundesministerium für Bildung und Forschung, Ministerium für Wissenschaft und Forschung des Landes Nordrhein-Westfalen, German–Israeli-Foundation, European Communities (Brite-Euram), Fonds der Chemischen Industrie, Engineering and Physical Sciences Research Council.

References

- [1] K. Weissermel and H.-J. Arpe, *Industrielle Organische Chemie* (Verlag Chemie, Weinheim, 1976).
- [2] *Handbook of Chemistry and Physics*, 54th ed. (CRC Press, Boca Raton, FL, 1973).
- [3] S. Inoue and N. Yamazaki, Eds., *Organic and Bio-Organic Chemistry of Carbon Dioxide* (Kodansha/Wiley, 1982).
- [4] A. Behr, *Carbon Dioxide Activation by Metal Complexes* (Verlag Chemie, Weinheim, 1988).
- [5] T. Andrews and G.H. Lorimer, in: *The Biochemistry of Plants*, Vol. 10, Eds. M.D. Hazch and N.K. Boardman (Academic Press, New York, 1987) p. 132.
- [6] J. Paul and C.-M. Pradier, Eds., *Carbon Dioxide Chemistry: Environmental Issues*, Spec. Publ. No. 153 (Roy Soc. of Chem., London, 1994).
- [7] W.A. Ayers, Ed., *Catalytic Activation of Carbon dioxide*, ACS Symp. Ser. 363 (Am. Chem. Soc., Washington, 1988).
- [8] F. Solymosi, *J. Mol. Catal.* 65 (1991) 337.
- [9] C.M. Quinn and M.W. Roberts, *Trans. Faraday Soc.* 59 (1963) 985.
- [10] S.J. Atkinson, C.R. Brundle and M.W. Roberts, *J. Electron Spectrosc. Rel. Phen.* 2 (1973) 105.
- [11] S.J. Atkinson, C.R. Brundle and M.W. Roberts, *Disc. Faraday Soc.* 58 (1974) 62.
- [12] A.T. Ashcroft, A.K. Cheetham, M.L.H. Green and P.D.F. Vernon, *Nature* 225 (1991) 352.
- [13] J.T. Richardson and S.A. Paripatyador, *Appl. Catal.* 61 (1990) 293.
- [14] N. Ikehara, K. Hara, A. Satsuma, T. Hattori and Y. Murakami, *Chem. Lett.* (1994) 263.
- [15] M. Kurioka, K. Nakata, T. Jintoku, Y. Taniguchi, K. Takaki and Y. Fujiwara, *Chem. Lett.* (1995) 244.
- [16] N.R. Udengaard, J.B. Hansen, D.C. Hansen and J.A. Stal, *Oil Gas J.* 62 (1992) 9.
- [17] G. Kurz and S. Teuner, *Erd. Kohle* 43 (1990) 171.
- [18] T. Inui, T. Takeguchi, A. Kohama and K. Tanida, *Energy Consers. Mgmt.* 33 (1992) 513.
- [19] G. Herzberg, *Electronic Spectra of Polyatomic Molecules* (Van Nostrand, New York, 1966).
- [20] W.L. Jorgensen and L. Salem, *Orbitale organischer Moleküle* (Verlag Chemie, Weinheim, 1974).
- [21] A.D. Walsh, *J. Chem. Soc.* (1953) 2260.
- [22] N.W. Winter, C.F. Bender and W.A. Goddard, *Chem. Phys. Lett.* 10 (1973) 489.

- [23] M.J. Hubin-Franskin and J.E. Collin, *Bull. Soc. Roy. Sci. Liege* 40 (1971) 361.
- [24] D.W. Turner, A.D. Baker, C. Baker and C.R. Brundle, *Molecular Photoelectron Spectroscopy* (Wiley, New York, 1970).
- [25] A.A. Radzig and B.M. Smirnov, *Reference Data on Atoms, Molecules, and Ions*, Springer Series in Chemical Physics, Vol. 31 (Springer, Berlin, 1984).
- [26] R.N. Compton, P.W. Reinhardt and C.D. Cooper, *J. Chem. Phys.* 63 (1975) 3821.
- [27] C.D. Cooper and R.N. Compton, *Chem. Phys. Lett.* 14 (1972) 29.
- [28] C.D. Cooper and R.N. Compton, *J. Chem. Phys.* 59 (1973) 3550.
- [29] D.W. Ovenall and D.H. Whiffen, *Mol. Phys.* 4 (1961) 135.
- [30] K.O. Hartmann and I.C. Hisatsume, *J. Chem. Phys.* 44 (1966) 1913.
- [31] J. Pacansky, K. Wahlgren and P.S. Bagus, *J. Chem. Phys.* 62 (1975) 2740.
- [32] M.J.W. Boness and G.J. Schulz, *Phys. Rev. A* 9 (1974) 1969.
- [33] M.E. Jacox and W.E. Thompson, *J. Chem. Phys.* 91 (1989) 1410.
- [34] H.-J. Freund and R.P. Messmer, *Surf. Sci.* 172 (1986) 1.
- [35] H.-J. Freund, H. Kossmann and V. Schmidt, *Chem. Phys. Lett.* 123 (1986) 463.
- [36] J.-H. Fock, H.-J. Lau and E.E. Koch, *Chem. Phys.* 83 (1984) 377.
- [37] J.-H. Fock, PhD Thesis, Universität Hamburg (1983).
- [38] W. Domcke, L.S. Cederbaum, J. Schirmer, W. von Niessen, C.E. Brion and K.H. Tan, *Chem. Phys.* 40 (1979) 171.
- [39] B. Bartos, H.-J. Freund, H. Kühlenbeck, M. Neumann, H. Linder and K. Müller, *Surf. Sci.* 179 (1987) 59.
- [40] A. Behr, *Angew. Chem.* 100 (1988) 681.
- [41] M. Aresta, C.F. Nobile, V.G. Albano, E. Forni and M. Manassero, *J. Chem. Soc., Chem. Commun.* (1975) 636.
- [42] M. Aresta and C.F. Nobile, *J. Chem. Soc. Dalton Trans.* (1977) 708.
- [43] W. Beck, K. Raab, U. Nagel and M. Steimann, *Angew. Chem.* 94 (1982) 526.
- [44] J.C. Calabrese, T. Herskovitz and J.B. Kinney, *J. Am. Chem. Soc.* 105 (1983) 5914.
- [45] S. Sakaki, K. Kitaura and K. Morokuma, *Inorg. Chem.* 21 (1982) 760.
- [46] R. Caballol, E.S. Marcos and J.-C. Barthelat, *J. Phys. Chem.* 91 (1987) 1328.
- [47] G.H. Jeung, *Mol. Phys.* 65 (1988) 669.
- [48] J.O. Hirschfelder, C.F. Curtiss and R.B. Bird, *Molecular Theory of Gases and Liquids* (Wiley, New York, 1954).
- [49] J.M. Lobue, J.K. Rice and S.E. Novick, *Chem. Phys. Lett.* 112 (1984) 376.
- [50] M.A. Johnson, M.L. Alexander and W.C. Lineberger, *Chem. Phys. Lett.* 112 (1984) 112.
- [51] N. Brigot, S. Odier, S.H. Walmsley and J.L. Whitten, *Chem. Phys. Lett.* 49 (1977) 157.
- [52] E.L. Quitevas and D.R. Herschbach, as referenced in K.H. Bowen, G.W. Liesegang, R.A. Sanders and D.R. Herschbach, *J. Phys. Chem.* 87 (1983) 557.
- [53] A.R. Rossi and K.D. Jordan, *J. Chem. Phys.* 70 (1979) 4422.
- [54] R.P. Eischens and W.A. Pliskin, *Adv. Catal.* 12 (1957) 662.
- [55] G. Blyholder and L.D. Neff, *J. Phys. Chem.* 66 (1962) 1464.
- [56] B.M. Gatehouse, S.E. Livingstone and R.S. Nyholm, *J. Chem. Soc.* (1958) 3137.
- [57] J. Fujita, A.E. Martell and K. Nakamoto, *J. Chem. Phys.* 36 (1962) 339.
- [58] L.H. Little, *Infrared Spectra of Adsorbed Species* (Academic Press, London, 1986).
- [59] J.H. Taylor and C.H. Amberg, *Can. J. Chem.* 39 (1961) 535.
- [60] L.H. Little and C.H. Amberg, *Can. J. Chem.* 40 (1962) 1997.
- [61] C.E. O'Neill and D.J.C. Yates, *Spectrochim. Acta* 17 (1961) 953.
- [62] A.D. Crowell and H.E. Farnsworth, *J. Chem. Phys.* 19 (1951) 1206.
- [63] J.A. Feighan and K.A. Krieger, in: *Proc. 2nd Int. Congr. on Catalysis, Paris, 1960*, p. 1027.
- [64] A.C. Collins and B.M.W. Trapnell, *Trans. Faraday Soc.* 53 (1957) 1476.
- [65] D.O. Hayward and R. Gomer, *J. Chem. Phys.* 30 (1959) 1617.
- [66] R.P. Eischens and W.A. Pliskin, in: *Proc. 2nd Int. Congr. on Catalysis, Paris, 1960*, p. 2005.
- [67] C.M. Quinn and M.W. Roberts, *Trans. Farad. Soc.* 58 (1962) 569.
- [68] R. Suhrmann, G. Schwandt and G. Wedler, *Z. Phys. Chem. (NF)* 35 (1962) 47.
- [69] C.R. Brundle and M.W. Roberts, *Proc. R. Soc. A* 331 (1972) 383.
- [70] K. Heinz, *Progr. Surf. Sci.* 27 (1988) 239.
- [71] S.D. Kevan, Ed., *Angle resolved photoemission: theory and current applications*, in: *Studies in Surface Science and Catalysis*, Vol. 74 (Elsevier, Amsterdam, 1992).

- [72] J. Stöhr, NEXAFS spectroscopy, in: Springer Series in Surface Science, Vol. 25 (Springer, Heidelberg, 1993).
- [73] H. Ibach and D.L. Mills, Electron Energy Loss Spectroscopy and Surface Vibrations (Academic Press, New York, 1982).
- [74] H. Behner, W. Spiess, G. Wedler and D. Borgmann, Surf. Sci. 175 (1986) 276.
- [75] H.-J. Freund, H. Behner, B. Bartos, G. Wedler, H. Kühlenbeck and M. Neumann, Surf. Sci. 180 (1987) 550.
- [76] G. Hess, H. Froitzheim and Ch. Baumgartner, Surf. Sci. 331–333 (1995) 138.
- [77] G. Illing, D. Heskett, E.W. Plummer, H.-J. Freund, J. Somers, Th. Lindner, A.M. Bradshaw, U. Buskotte, M. Neumann, U. Starke, K. Heinz, P.L. De Andres, D. Saldin and J.B. Pendry, Surf. Sci. 206 (1988) 1.
- [78] M.D. Crapper, C.E. Riley, D.P. Woodruff, A. Puschmann and J. Haase, Surf. Sci. 171 (1986) 1.
- [79] D.P. Woodruff, C.F. McConville, A.L.D. Kilcoyne, Th. Lindner, J. Somers, M. Surman, G. Paolucci and A.M. Bradshaw, Surf. Sci. 201 (1988) 228.
- [80] J. Wambach, G. Illing and H.-J. Freund, Chem. Phys. Lett. 184 (1991) 239.
- [81] T.S. Jones, M.R. Ashton and N.V. Richardson, J. Chem. Phys. 90 (1989) 7564.
- [82] R.J. Madix, J.L. Solomon and J. Stöhr, Surf. Sci. 197 (1988) L253.
- [83] E.M. Stuve, R.J. Madix and B.A. Sexton, Chem. Phys. Lett. 89 (1982) 48.
- [84] C. Backx, C.P.M. de Groot, P. Biloen and W.M.H. Sachtler, Surf. Sci. 128 (1983) 81.
- [85] V.L. Borodin, V.I. Lyutin, V.V. Ilyukin and N.V. Belov, Sov. Phys. Dokl. 24 (1979) 226.
- [86] M.A. Barteau and R.J. Madix, J. Electron Spectrosc. Rel. Phen. 31 (1983) 101.
- [87] C.T. Au and M.W. Roberts, Proc. R. Soc. London A 396 (1984) 165.
- [88] S. Campbell, P. Hollins, E. McCash and M.W. Roberts, J. Electron Spectrosc. Rel. Phen. 39 (1986) 145.
- [89] A.F. Carley, D.E. Gallagher and M.W. Roberts, Surf. Sci. 183 (1987) L263.
- [90] A.F. Carley, D.E. Gallagher and M.W. Roberts, Spectrochim. Acta A 43 (1987) 1447.
- [91] V.M. Browne, A.F. Carley, R.G. Copperthwaite, P.R. Davies, E.M. Moser and M.W. Roberts, Appl. Surf. Sci. 47 (1991) 375.
- [92] M. Bowker, M.A. Barteau and R.J. Madix, Surf. Sci. 92 (1980) 528.
- [93] M. Sakurai, T. Okano and Y. Tuzi, J. Vac. Sci. Technol. A 5 (1987) 431.
- [94] T.H. Ellis, G. Scoles, U. Valbusa, H. Jönsson and J.H. Weare, Surf. Sci. 155 (1985) 499.
- [95] M.A. Barteau and R.J. Madix, J. Chem. Phys. 74 (1981) 4144.
- [96] A.W. Czanderna, J. Coll. Interf. Sci. 22 (1966) 482.
- [97] A.W. Czanderna, J. Phys. Chem. 70 (1966) 2120.
- [98] A.W. Czanderna and J.R. Biegen, J. Vac. Sci. Technol. 8 (1971) 594.
- [99] M.W. Roberts, Chem. Soc. Rev. 18 (1989) 451.
- [100] M.W. Roberts and R.G. Copperthwaite (unpublished data see Ref. [99]).
- [101] J. Paul, Nature 323 (1986) 701.
- [102] J. Paul and F.M. Hoffmann, Catal. Lett. 1 (1988) 445.
- [103] W. Akemann and A. Otto, Surf. Sci. 272 (1992) 211.
- [104] W. Akemann and A. Otto, Surf. Sci. 287/288 (1993) 104.
- [105] G.C. Chinchin, P.J. Denny, D.G. Parker, M.S. Spencer and D.A. Whan, Appl. Catal. 30 (1987) 333.
- [106] R.G. Copperthwaite, P.R. Davies, M.A. Morris, M.W. Roberts and R.A. Ryder, Catal. Lett. 1 (1988) 11.
- [107] G.C. Chinchin, M.S. Spencer, K.C. Waugh and D.A. Whan, J. Chem. Soc. Faraday Trans. I, 83 (1987) 2193.
- [108] B. Rasmussen, P.A. Taylor and I. Chorkendorff, Surf. Sci. 269/270 (1992) 352.
- [109] P.B. Rasmussen, M. Kazuta and I. Chorkendorff, Surf. Sci. 318 (1994) 267.
- [110] P.A. Taylor, P.B. Rasmussen and I. Chorkendorff, J. Vac. Sci. Technol. A 10 (1992) 2570.
- [111] J.A. Rodriguez, W.D. Clendening and C.T. Campbell, J. Phys. Chem. 93 (1989) 5238.
- [112] J. Krause, D. Borgmann and G. Wedler, Surf. Sci. 347 (1996) 1.
- [113] L. Bugyi, J. Kiss and F. Solymosi, as referenced in [8].
- [114] S.S. Fu and G.A. Somorjai, Surf. Sci. 262 (1992) 68.
- [115] I. Bönicke, W. Kirstein and F. Thieme, Surf. Sci. 307 (1994) 177.
- [116] I.E. Wachs and R.J. Madix, J. Catal. 53 (1978) 208.
- [117] A.F. Carley, M.W. Roberts and A.J. Strutt, J. Phys. Chem. 98 (1994) 9175.
- [118] A.F. Carley, M.W. Roberts and A.J. Strutt, Catal. Lett. 29 (1994) 169.
- [119] J. Onsgaard, J. Storm, S.V. Christensen, J. Nerlov, P.J. Godowski, P. Morgen and D. Batchelor, Surf. Sci. 336 (1995) 101.

- [120] E.V. Thomsen, B. Jørgensen and J. Onsgaard, *Surf. Sci.* 304 (1994) 85.
- [121] R. Dziembaj and G. Wedler, *Surf. Sci.* 134 (1983) 283.
- [122] R. Bauer, H. Behner, D. Borgmann, M. Pirner, W. Spiess and G. Wedler, *J. Vac. Sci. Technol. A* 5 (1987) 1110.
- [123] A. Erdöhelyi, E. Anneser, Th. Bauer, K. Stephan, D. Borgmann and G. Wedler, *Surf. Sci.* 227 (1990) 57.
- [124] M.H. Nassir and D.J. Dwyer, *J. Vac. Sci. Technol. A* 11 (1993) 2104.
- [125] R. Yoshida and G. Somorjai, *Surf. Sci.* 75 (1978) 46.
- [126] J. Paul, *Surf. Sci.* 224 (1989) 348.
- [127] G. Meyer, E. Reinhart, D. Borgmann and G. Wedler, *Surf. Sci.* 320 (1994) 110.
- [128] G. Meyer, D. Borgmann and G. Wedler, *Surf. Sci.* 320 (1994) 123.
- [129] T. Matsushima, Y. Ohno and K. Nagai, *Surf. Sci.* 239 (1990) L561.
- [130] Y. Ohno, T. Matsushima and H. Miki, *Surf. Sci.* 281 (1993) 234.
- [131] J.B. Benzinger and R.J. Madix, *Surf. Sci.* 79 (1979) 394.
- [132] M.P. D'Evelyn, A.V. Hamza, G.E. Gdowski and R.J. Madix, *Surf. Sci.* 167 (1986) 451.
- [133] H. Lindner, D. Rupprecht, L. Hammer and K. Müller, *J. Electron Spectrosc. Rel. Phen.* 44 (1987) 141.
- [134] W. Heiland, *Surf. Sci.* 251/252 (1991) 942.
- [135] R.J. Behm and C.R. Brundle, *Surf. Sci.* 255 (1991) 327.
- [136] R.J. Behm and C.R. Brundle, *J. Vac. Sci. Technol. A* 1 (1983) 1223.
- [137] D.E.A. Gordon and R.M. Lambert, *Surf. Sci.* 287/288 (1993) 114.
- [138] F. Solymosi and A. Berkó, *J. Catal.* 101 (1986) 458.
- [139] D. Ehrlich, S. Wohlrab, J. Wambach, H. Kuhlenbeck and H.-J. Freund, *Vacuum* 41 (1990) 157.
- [140] S. Wohlrab, D. Ehrlich, J. Wambach, H. Kuhlenbeck and H.-J. Freund, *Surf. Sci.* 220 (1990) 243.
- [141] J. Wambach, G. Odörfer, H.-J. Freund, H. Kuhlenbeck and M. Neumann, *Surf. Sci.* 209 (1989) 159.
- [142] T. Matsushima, *J. Phys. Chem.* 91 (1987) 6192.
- [143] A. Berkó and F. Solymosi, *Surf. Sci.* 171 (1986) L498.
- [144] T. Schlathölter and W. Heiland, *Surf. Sci.* 323 (1995) 207.
- [145] P.R. Norton, *Surf. Sci.* 44 (1974) 624.
- [146] P.R. Norton and P.J. Richards, *Surf. Sci.* 49 (1975) 567.
- [147] M.F.H. van Tol, A. Gielbert, R.M. Wolf, A.B.K. Lie and B.E. Nieuwenhuys, *Surf. Sci.* 287/288 (1993) 201.
- [148] J. Segner, C.T. Campbell, G. Doyen and G. Ertl, *Surf. Sci.* 138 (1984) 505.
- [149] C.T. Campbell, G. Ertl, H. Kuipers and J. Segner, *J. Chem. Phys.* 73 (1980) 5862.
- [150] Z.M. Liu, Y. Zhou, F. Solymosi and J.M. White, *J. Phys. Chem.* 93 (1989) 4383.
- [151] Z.M. Liu, Y. Zhou, F. Solymosi and J.M. White, *Surf. Sci.* 245 (1991) 289.
- [152] H. Peled and M. Asscher, *Surf. Sci.* 183 (1987) 201.
- [153] H. Asscher, C.-T. Kao and G.A. Somorjai, *J. Phys. Chem.* 92 (1988) 2711.
- [154] J.A. Rodriguez, R.A. Campbell and D.W. Goodman, *Surf. Sci.* 244 (1991) 211.
- [155] C.T. Campbell and J.M. White, *J. Catal.* 54 (1978) 289.
- [156] A.C. Yang and C.W. Garland, *J. Phys. Chem.* 61 (1957) 1504.
- [157] F. Solymosi and J. Kiss, *Surf. Sci.* 149 (1985) 17.
- [158] F. Solymosi and J. Kiss, *Chem. Phys. Lett.* 110 (1984) 639.
- [159] F. Solymosi and L. Bugyi, *J. Chem. Soc. Faraday Trans. I*, 83 (1987) 2015.
- [160] F. Solymosi and G. Klivényi, *Catal. Lett.* 22 (1993) 337.
- [161] J. Kiss, K. Révész and F. Solymosi, *Surf. Sci.* 207 (1988) 36.
- [162] F. Solymosi and G. Klivényi, *J. Phys. Chem.* 98 (1994) 8061.
- [163] F. Solymosi and G. Klivényi, *Surf. Sci.* 315 (1994) 255.
- [164] F.M. Hoffmann, M.D. Weisel and J. Paul, *Surf. Sci.* 316 (1994) 277.
- [165] Z.H. Kafafi, R.H. Hange, W.E. Billups and J.L. Margrave, *J. Am. Chem. Soc.* 105 (1983) 3886.
- [166] L.H. Dubois and G.A. Somorjai, *Surf. Sci.* 128 (1983) L231.
- [167] W.H. Weinberg, *Surf. Sci.* 128 (1983) L224.
- [168] D.W. Johnson, M.H. Matloob and M.W. Roberts, *J. Chem. Soc. Faraday Trans. I*, 75 (1979) 2143.
- [169] A.F. Carley, M.K. Rajumon and M.W. Roberts, to be published.
- [170] P.R. Davies and M.W. Roberts, *J. Chem. Soc. Faraday Trans. I*, 88 (1992) 361.

- [171] C.T. Campbell and K.-H. Ernst, in: *Surface Science of Catalysis*, ACS Symp. 482, Eds. D.J. Dwyer and F.M. Hoffmann, 1992, p. 130.
- [172] D. Mueller, A. Shih, E. Roman, T. Madey, R. Kurtz and R. Stockbauer, *J. Vac. Sci. Technol. A* 6 (1988) 1067.
- [173] G. Pacchioni, J.M. Ricart and F. Illas, *J. Am. Chem. Soc.* 116 (1994) 10 152.
- [174] H. Kühlenbeck, C. Xu, B. Dillmann, M. Haßel, B. Adam, D. Ehrlich, S. Wohlrab, H.-J. Freund, U.A. Ditzinger, H. Neddermeyer, M. Neuber and M. Neumann, *Ber. Bunsenges. Phys. Chem.* 96 (1992) 15.
- [175] B. Dillmann, O. Seiferth and H.-J. Freund, unpublished data.
- [176] V.M. Allen, W.E. Jones and P.D. Pacey, *Surf. Sci.* 199 (1988) 309.
- [177] J. Heidberg and D. Meine, *Surf. Sci.* 279 (1992) L175.
- [178] J. Heidberg, D. Meine and B. Redlich, *J. Electron Spectrosc. Rel. Phen.* 64/65 (1993) 599.
- [179] D.L. Meixner, D.A. Arthur and S.M. George, *Surf. Sci.* 261 (1992) 141.
- [180] J. Suzanne, V. Panella, D. Ferry and M. Sidoumou, *Surf. Sci.* 293 (1993) L912.
- [181] G. Pacchioni, *Surf. Sci.* 281 (1993) 207.
- [182] H. Onishi, C. Egawa, T. Aruga and Y. Iwasawa, *Surf. Sci.* 191 (1987) 479.
- [183] H. Onishi, T. Aruga and Y. Iwasawa, *Surf. Sci.* 310 (1994) 135.
- [184] A. Boudriss and L.C. Dufour, in: *Non-Stoichiometric Compounds: Surfaces, Grain, Boundaries and Structural Defects*, Eds. J. Nowotny and W. Weppner (Kluwer, Dordrecht, 1989) p. 311.
- [185] W. Göpel and G. Rucker, *J. Vac. Sci. Technol.* 21 (1982) 389.
- [186] W. Göpel, G. Rucker and R. Feierabend, *Phys. Rev. B* 28 (1983) 3427.
- [187] M. Watanabe, *Surf. Sci.* 279 (1992) L236.
- [188] W. Göpel, R.S. Bauer and G. Hansson, *Surf. Sci.* 99 (1980) 138.
- [189] W. Göpel, *Prog. Surf. Sci.* 20 (1985) 9.
- [190] F. Runge and W. Göpel, *Z. Phys. Chem.* 123 (1980) 173.
- [191] W. Hotan, W. Göpel and R. Haul, *Surf. Sci.* 83 (1979) 162.
- [192] S.F. Jen and A.B. Anderson, *Surf. Sci.* 223 (1989) 119.
- [193] W.H. Cheng and H.H. Kung, *Surf. Sci.* 102 (1981) L21.
- [194] W.H. Cheng and H.H. Kung, *Surf. Sci.* 122 (1982) 21.
- [195] C.T. Au, W. Hirsch and W. Hirschwald, *Surf. Sci.* 199 (1988) 507.
- [196] R. Davis, J.F. Walsh, C.A. Muryn, G. Thornton, V.R. Dhanak and K.C. Prince, *Surf. Sci.* 298 (1993) L196.
- [197] C.T. Au, W. Hirsch and W. Hirschwald, *Surf. Sci.* 197 (1988) 391.
- [198] J.A. Rodriguez, *Langmuir* 4 (1988) 1006.
- [199] P.J. Møller, S.A. Komolov, E.F. Lazneva and E.H. Pedersen, *Surf. Sci.* 323 (1995) 102.
- [200] J. Heidberg, E. Kampshoff, R. Kühnemuth and O. Schönekas, *J. Electron Spectrosc. Rel. Phen.* 64/65 (1993) 803.
- [201] J. Heidberg, E. Kampshoff, R. Kühnemuth, O. Schönekas, H. Stein and H. Weiss, *Surf. Sci.* 226 (1990) L43.
- [202] J. Heidberg, E. Kampshoff, R. Kühnemuth and O. Schönekas, *Surf. Sci.* 251/252 (1991) 314.
- [203] J. Heidberg, E. Kampshoff, R. Kühnemuth and O. Schönekas, *Surf. Sci.* 269/270 (1992) 120.
- [204] J. Heidberg, E. Kampshoff, R. Kühnemuth and O. Schönekas, *Surf. Sci.* 272 (1992) 306.
- [205] J. Heidberg, E. Kampshoff, R. Kühnemuth, O. Schönekas, G. Lange, D. Schmicker, J.P. Toennies, R. Vollmer and H. Weiss, *J. Electron Spectrosc. Rel. Phen.* 64/65 (1993) 341.
- [206] O. Berg, R. Disselkamp and G.E. Ewing, *Surf. Sci.* 277 (1992) 8.
- [207] K. Tanabe, in: *Catalysis—Science and Technology*, Eds. J.R. Anderson and M. Boudart (Springer, Berlin, 1981) p. 123.
- [208] A.F. Carley, P.R. Davies, E. Moser and M.W. Roberts, *Surf. Sci.*, in press.
- [209] J. Wambach, PhD Thesis, Ruhr-Universität Bochum (1991).
- [210] J. Wambach and H.-J. Freund, in: *Carbon Dioxide Chemistry: Environmental Issues*, Eds. J. Paul and C.-M. Pradier, The Royal Society of Chemistry Special Publ. No. 153 (1994) p. 31.
- [211] R. Burch, S. Chalker and J. Pritchard, *J. Chem. Soc. Faraday Trans. I*, 87 (1991) 193.
- [212] P.A. Taylor P.B. Rasmussen, C.V. Ovesen, P. Stoltze and I. Chorkendorff, *Surf. Sci.* 261 (1992) 191.
- [213] H.P. Bonzel, *Surf. Sci. Rep.* 8 (1988) 43.
- [214] G.U. Kulkarni, S. Laruelle and M.W. Roberts, *Chem. Commun.* (1996) 9.
- [215] K.J. Maynard and M. Moskovits, *Surf. Sci.* 225 (1990) 40.